Supplementary Information

Structural diversity of new solid-state luminophores based on quinoxaline-*β*-ketoiminate boron difluoride complexes with remarkable fluorescence switching properties

Chia-Wei Liao, Rajeswara Rao M, and Shih-Sheng Sun*

Institute of Chemistry, Academia Sinica, Taipei, Taiwan, Republic of China.

E-mail: sssun@chem.sinica.edu.tw

Experimental Section:

General procedures and instrumentation:

All chemical reagents were commercially available and were used without further purification. All reactions were monitored using pre-coated TLC plates and purified by column chromatography. Column chromatography was performed on silica (60-120 mesh). Absorption and fluorescence spectra were obtained with a Varian Cary 300 UV-vis spectrophotometer and a Jobin-Yvon FL3-21 Horiba fluorolog fluorimeter, respectively. Fluorescence quantum yields were measured by using 9, 10-diphenylanthracence (DPA) in cyclohexane (95%) or Rhodamine 6G in ethanol (94%) as a standard reference and solid-state emission quantum yields were determined by the Jobin-Yvon FL3-21 Horiba fluorolog fluorimeter equipped with an integrated sphere. The time-resolved fluorescence decay measurements were carried out on Edinburgh Photonics Model FLS920 with a picosecond pulsed diode laser as an excitation source. The decay time fitting procedure was carried out with the IRF by using the fitting program and all of the decays were fitted to a single exponential. ^{1}H, ^{13}C, ^{11}B, and ^{19}F NMR spectra were recorded by using Bruker AVANCE III 400 MHz, Ultra Shield 400 and 500 MHz NMR. The HR-MALDI mass spectra were conducted on an Applied Biosystems 4800 Proteomics Analyzer equipped with an Nd/YAG laser (335nm) operating at a repetition rate of 200 Hz. The HR-EI mass spectra were conducted on a JMS-700 double focusing mass spectrometer (JEOL, Tokyo, Japan) with a resolution of 8000(3000) (5% valley definition). Cyclic voltammetry (CV) and differential pulse voltammetry (DPV) studies were carried out on CHI Model 621B Electrochemical Analyzer with a three-electrode configuration consisting of a platinum working electrode, a platinum wire auxiliary electrode, and a non-aqueous $Ag/AgNO_3$ reference electrode. The experiments were performed in degassed CH_2Cl_2 containing 0.1 M $TBAPF_6$ (tetrabutylammonium hexafluorophosphate) and 1.0 mM of the compound. The potentials were quoted against the ferrocene$^{+1/0}$ redox couple as the internal standard

and converted to NHE by addition of 0.63 V. Crystallographic X-ray data were collected by using a Bruker Nonius Kappa CCD diffractometer with Mo K_{α} radiation.

General procedures for the synthesis of ligands **1a-5a:**

Sodium hydride (60 w% in oil, 2.4 g, 60 mmol) was added to a solution of the quinoxaline precursor (**6-8**, 20 mmol) and corresponding methyl benzoate (23 mmol) in dry THF (50 mL) at room temperature. The solution was refluxed for 1 day. After cooling to room temperature, the solution was added to ammonium chloride aqueous solution (100 mL) and then extracted with dichloromethane. The organic phase was dried over $MgSO_4$, filtered, and evaporated under reduced pressure. The residue was further purified by column chromatography (dichloromethane/n-hexane = 2:3) to yield the desired product as a solid powder.

1a: Yield: 85%; a dark-red powder; m.p. 123–124 °C. ^{1}H NMR (400 MHz, $CDCl_3$, δ in ppm): 14.74 (bs, 1H), 8.47 (s, 1H), 7.97–7.94 (m, 2H), 7.86–7.84 (d, J = 10.8 Hz, 1H), 7.61–7.39 (m, 6H), 6.28 (s, 1H). ^{13}C NMR (125 MHz, $CDCl_3$, δ in ppm): 181.9, 149.9, 148.1, 137.9, 137.7, 133.0, 131.3, 131.2, 129.4, 128.7, 126.7, 125.9, 120.1, 91.4. HRMS (EI): m/z calcd for $C_{16}H_{12}ON_2$: 248.0950 $[M]^+$; found: 248.0955.

2a: Yield: 69%; a yellow powder; m.p. 120–121°C. ^{1}H NMR (400 MHz, $CDCl_3$, δ in ppm): 15.61 (bs, 1H), 7.97 (dd, J = 7.2, 1.6 Hz, 2H), 7.78 (d, J = 8.0 Hz, 1H), 7.53–7.44 (m, 5H), 7.37 (t, J = 7.4 Hz, 1H), 6.30 (s, 1H), 2.65 (s, 3H). ^{13}C NMR (125 MHz, $CDCl_3$, δ in ppm): 184.9, 155.7, 147.0, 139.1, 136.4, 131.2, 131.1, 130.2, 128.7, 128.6, 127.0, 125.4, 118.5, 88.5, 22.6. HRMS (EI): m/z calcd for $C_{17}H_{14}ON_2$: 262.1106 $[M]^+$; found: 262.1104.

3a: Yield: 71%; an orange powder; m.p. 128–129 °C. ^{1}H NMR (400 MHz, $CDCl_3$, δ in ppm): isomer (enol : keto = 3 : 1). Enol form: 15.48 (bs, 1H), 7.84 (d, J = 8.8 Hz, 2H), 7.74 (d, J = 8.0 Hz, 1H), 7.33–7.29 (m, 6H), 7.16 (d, J = 8.0 Hz, 6H), 7.13–7.06 (m, 3H), 6.23 (s, 1H), 2.61 (s, 3H). Keto form: 8.02 (t, J = 7.6 Hz, 2H), 7.93 (d, J = 8.8 Hz, 2H), 7.68 (t, J = 7.0 Hz, 2H), 7.48 (t, J = 7.8 Hz, 3H), 7.39 (d, J = 8.0 Hz, 3H), 7.33–7.29 (m, 3H), 7.13–7.06 (m, 2H), 7.01–6.98 (m, 1H), 4.69 (s, 2H), 2.73 (s, 3H). ^{13}C NMR (125 MHz, $CDCl_3$, δ in ppm): 185.0, 156.0, 152.9, 150.9, 147.1, 146.7, 146.4, 135.5, 133.1, 131.6, 131.1, 130.3, 129.9, 129.7, 128.7, 128.3, 126.6, 126.4, 126.1, 125.7, 125.0, 124.8, 124.3, 121.1, 119.9, 119.4, 119.0, 118.8, 117.9, 88.0, 46.5, 29.8, 22.4. HRMS (MALDI): m/z calcd for $C_{29}H_{24}ON_3$: 430.1919 $[M+H]^+$; found: 430.1937.

4a: Yield: 81%; a yellow powder; m.p. 138–139 °C. ^{1}H NMR (400 MHz, $CDCl_3$, δ in ppm): 15.83 (bs, 1H), 7.92 (d, J = 8.0 Hz, 1H), 7.80 (d, J = 7.2 Hz, 2H), 7.76 (d, J = 8.0 Hz, 2H), 7.58–7.56 (m, 5H), 7.46–7.39 (m, 4H), 6.40 (s, 1H). ^{13}C NMR (125 MHz, $CDCl_3$, δ in ppm): 181.5, 157.0, 147.8, 138.3, 137.5, 137.4, 131.0, 130.9, 129.9, 129.5, 129.0, 128.9, 128.8, 128.6, 126.7, 126.1, 119.8, 91.4. HRMS (MALDI): m/z calcd for $C_{22}H_{17}O\ N_2$: 325.1341 $[M+H]^+$; found: 325.1349.

5a: Yield: 79%; an orange powder; m.p. 126–127 °C. ^{1}H NMR (400 MHz, $CDCl_3$, δ in ppm): isomer (enol : keto = 5 : 1). Enol form: 15.67 (bs, 1H), 7.77–7.72 (m, 2H), 7.65 (d, J = 8.8 Hz, 2H), 7.60–7.44 (m, 5H), 7.34–7.30 (m, 6H), 7.16–7.07 (m, 6H), 6.99 (d, J = 8.0 Hz, 2H), 6.29 (s, 1H). Keto form: 7.85 (d, J = 8.4 Hz, 2H), 7.77–7.72 (m, 2H), 7.60–7.44 (m, 5H), 7.39–7.35 (m, 6H), 7.16–7.07 (m, 6H), 6.93 (d, J = 8.4 Hz, 2H), 4.67 (s, 2H). ^{13}C NMR (125 MHz, $CDCl_3$, δ in ppm): 182.4, 157.43, 150.8, 147.0, 137.5, 136.8, 132.2, 132.0, 131.3, 130.8, 130.5, 130.5, 129.8, 129.7, 129.4, 129.2, 129.1, 128.9, 128.8,

128.1, 126.7, 126.5, 126.4, 126.1, 125.7, 125.3, 125.2, 124.2, 121.1, 118.9, 90.8, 45.8. HRMS (MALDI): *m*/*z* calcd for $C_{34}H_{26}N_3O$: 492.2076 $[M+H]^+$; found: 492.2088.

General procedures for the synthesis of organoboron difluoride complexes **1-5**

To a 100 mL $CHCl_3$ solution containing the ligand (**1a-5a**, 5 mmol) was added triethylamine (8.5 mL, 61.2 mmol) at room temperature. After stirring for 10 min, BF_3•OEt_2 (10 mL, 78.9 mmol) was added and the reaction was continued for 1 h. Completion of the reaction was monitored by TLC. The reaction mixture was evaporated and the crude product was purified *via* silica gel column chromatography (ethyl acetate/n-hexane=1:4) to afford the pure compound.

1: Yield: 92%; a deep green powder; m.p. 225–226 °C. ^{1}H NMR (400 MHz, $CDCl_3$, δ in ppm): 8.81 (s, 1H), 8.61 (d, J = 8.8 Hz, 1H), 8.09–8.05 (m, 3H), 7.83 (td, J = 8.0, 1.2 Hz, 1H), 7.70 (td, J = 7.6, 0.8 Hz, 1H), 7.58–7.47 (m, 3H), 6.58 (s, 1H). ^{11}B NMR (128 MHz, $CDCl_3$, ext. std. BF_3•Et_2O, δ inppm): 1.99 (t, J =16.2 Hz (B-F), 1B). ^{13}C NMR (125 MHz, $CDCl_3$, δ in ppm): 169.8, 147.5, 146.2, 141.3, 133.2, 132.9, 132.8, 131.3, 130.4, 129.0, 128.9, 127.5, 122.4, 92.1. ^{19}F NMR (376 MHz, $CDCl_3$, ext. std. $C_6H_5CF_3$, δ in ppm): –127.07 (q, J =16.2 Hz (F-B), 2F). HRMS (EI): *m*/*z* calcd for $C_{16}H_{11}ON_2F_2B$: 296.0932 $[M]^+$; found: 296.0931.

2: Yield: 83%; a yellow powder; m.p. 252–253 °C. ^{1}H NMR (400 MHz, $CDCl_3$, δ in ppm): 8.60 (d, J = 8.8 Hz, 1H), 8.06–8.04 (m, 2H), 7.89 (dd, J = 8.0, 1.6 Hz, 1H), 7.75 (td, J = 7.2, 1.6 Hz, 1H), 7.67 (t, J = 7.2 Hz, 1H), 7.54–7.47 (m, 3H), 6.64 (s, 1H), 2.87 (s, 3H). ^{11}B NMR (128 MHz, $CDCl_3$, ext. std. BF_3•Et_2O, δ in ppm): 2.09 (t, J =16.6 Hz (B-F), 1B). ^{13}C NMR (125 MHz, $CDCl_3$, δ in ppm): 169.5, 153.6, 145.9, 140.3, 133.5, 132.6, 131.6, 130.7, 129.6, 129.0, 128.8, 127.4, 122.3, 90.2, 23.5. ^{19}F NMR

(376 MHz, $CDCl_3$, ext. std. $C_6H_5CF_3$, δ in ppm): –127.43 (q, J =16.5 Hz (F-B), 2F). HRMS (EI): *m*/*z* calcd for $C_{17}H_{13}N_2BF_2$: 310.1089 $[M]^+$; found: 378.1086.

3: Yield: 79%; a brown powder; m.p. 221–222 °C. ^{1}H NMR (400 MHz, $CDCl_3$, δ in ppm): 8.53 (d, J = 8.4 Hz, 1H), 7.93 (d, J = 7.6 Hz, 1H), 7.90 (d, J = 8.8 Hz, 2H), 7.70 (t, J = 7.8 Hz, 1H), 7.60 (t, J = 7.6 Hz, 1H), 7.34 (t, J = 7.8 Hz, 4H), 7.19–7.14 (m, 6H), 7.04 (d, J = 8.8 Hz, 2H), 6.50 (s, 1H), 2.80 (s, 3H). ^{11}B NMR (128 MHz, $CDCl_3$, ext. std. BF_3•Et_2O, δ in ppm): 2.00 (t, J =16.3 Hz (B-F), 1B). ^{13}C NMR (125 MHz, $CDCl_3$, δ in ppm): 169.45, 153.72, 152.18, 146.50, 145.9, 139.6, 131.4, 130.9, 129.8 129.4, 129.0, 128.0, 126.2, 125.0, 122.0, 122.0, 120.2, 88.87, 23.47. ^{19}F NMR (376 MHz, $CDCl_3$, ext. std. $C_6H_5CF_3$, δ in ppm): –127.92 (q, J =16.5 Hz (F-B), 2F). HRMS (MALDI): *m*/*z* calcd for $C_{29}H_{23}ON_3BF_2$: 478.1924 $[M+H]^+$; found: 478.1902.

4: Yield: 82%; an orange powder; m.p. 215–216 °C. ^{1}H NMR (400 MHz, $CDCl_3$, δ in ppm): 8.67 (d, J = 8.8 Hz, 1H), 8.10 (d, J = 8.4 Hz, 1H), 7.88 (d, J = 7.6 Hz, 2H), 7.82 (t, J = 8.0 Hz, 1H), 7.73–7.69 (m, 3H), 7.63-7.61 (m, 3H), 7.51 (t, J = 7.2 Hz, 1H), 7.44 (t, J = 7.2 Hz, 2H), 6.70 (s, 1H). ^{11}B NMR (128 MHz, $CDCl_3$, ext. std. BF_3•Et_2O, δ in ppm): 2.19 (t, J =16.2 Hz (B-F), 1B). ^{13}C NMR (125 MHz, $CDCl_3$, δ in ppm): 169.0, 155.8, 145.8, 140.7, 136.9, 133.5, 132.5, 130.8, 130.4, 129.3, 129.2, 129.1, 128.9, 127.4, 122.4, 92.5. ^{19}F NMR (376 MHz, $CDCl_3$, ext. std. $C_6H_5CF_3$, δ in ppm): –127.33 (q, J =16.4 Hz (F-B), 2F). HRMS (MALDI): *m*/*z* calcd for $C_{22}H_{16}ON_2$ BF_2: 373.1324 $[M+H]^+$; found: 373.1334.

5: Yield: 91%; a dark-red powder; m.p. 257–258 °C. ^{1}H NMR (400 MHz, $CDCl_3$, δ in ppm): 8.60 (d, J = 8.8 Hz, 1H), 8.04 (dd, J = 8.0, 1.2 Hz, 1H), 7.76 (td, J = 7.8, 1.2 Hz, 1H), 7.71–7.68 (m, 4H), 7.73 (t, J = 7.8 Hz, 1H), 7.58–7.56 (m, 3H), 7.32 (t, J = 7.6 Hz, 4H), 7.15–7.12 (m, 6H), 6.97 (d, J = 8.8

Hz, 2H), 6.53 (s, 1H). ^{11}B NMR (128 MHz, $CDCl_3$, ext. std. BF_3•Et_2O, δ in ppm): 2.07 (t, J =17.0 Hz (B-F), 1B). ^{13}C NMR (125 MHz, $CDCl_3$, δ in ppm): 168.9, 156.0, 152.1, 146.5, 145.8, 140.0, 137.1, 132.2, 131.0, 130.3, 130.2, 129.8,129.2, 129.1, 128.9, 128.3, 126.2, 125.0, 122.0, 120.1, 91.3. ^{19}F NMR (376 MHz, $CDCl_3$, ext. std. $C_6H_5CF_3$, δ in ppm): –127.75 (q, J =17.3 Hz (F-B), 2F). HRMS (MALDI): m/z calcd for $C_{34}H_{24}ON_3BF_2$: 539.1981 $[M]^+$; found: 540.2018.

Table S1. Redox Data for complexes **1-5**[a]

Dyes	E_{ox}, V	E_{red}, V	$E_{0\text{-}0}$, eV[b]	E_{HOMO}, eV	E_{LUMO}, eV
1	1.48	–1.07	2.65	–6.28	–3.73
2	1.43	–1.14	2.69	–6.23	–3.66
3	0.63, 1.55	–1.20	2.25	–5.43	–3.60
4	1.52	–1.08	2.62	–6.32	–3.72
5	0.61, 1.56	–1.20	2.19	–5.41	–3.60

[a] All redox potentials (vs. Fc/Fc^+) were measured in CH_2Cl_2 with $TBAPF_6$ (0.1 M) as the supporting electrolyte (scan rate = 100 mV/s). E_{HOMO} and E_{LUMO} were derived from the electrochemical data.
[b] $E_{0\text{–}0}$ values were estimated from the intersection of the normalized absorption and emission spectra.

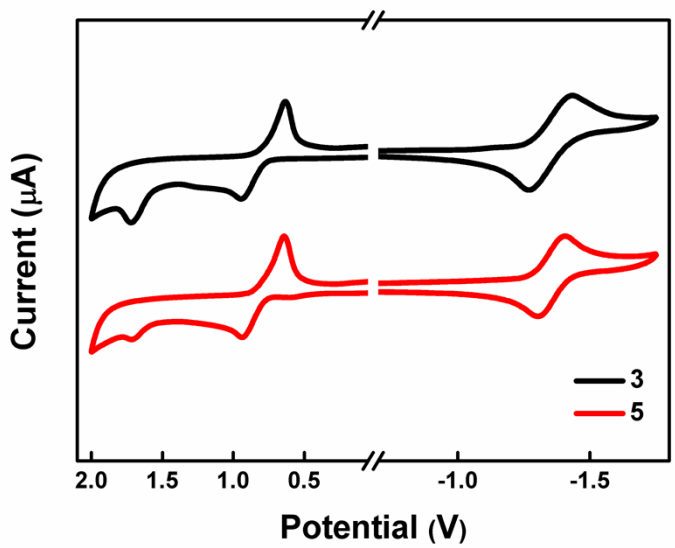

Fig. S1 Cyclic voltammograms of complexes **3** and **5**

Table S2. Optical Properties of **1-5**

dye	matrix	λ_{abs}, nm (log ε[a])	λ_{em}, nm	Δ (cm^{-1})	τ (ns)	Φ	k_r (10^8 s^{-1})	k_{nr} (10^7 s^{-1})

1	hexane	406 (4.28), 429 (4.50), 457 (4.49)	461	190	3.61	0.76	2.1	6.6
	toluene	409 (4.22), 433 (4.42), 459 (4.36)	475	733	4.05	0.79	2.0	5.2
	$CHCl_3$	410 (4.21), 434 (4.43), 459 (4.39)	475	733	4.13	0.92	2.2	1.9
	THF	409 (4.29), 430 (4.38), 455 (4.34)	476	988	4.16	0.71	1.7	6.9
	ACN	405 (4.23), 426 (4.39), 450 (4.34)	477	1257	4.41	0.85	1.9	3.4
	solid		580		0.18 (20%) 5.00 (80%)	0.020		
2	hexane	401 (4.24), 423 (4.46), 449 (4.43)	456	342	2.08	0.52	2.5	23.0
	toluene	404 (4.25), 427 (4.44), 452 (4.38)	468	756	2.86	0.70	2.4	10.5
	$CHCl_3$	405 (4.27), 427 (4.47), 452 (4.42)	467	711	2.75	0.81	2.9	6.9
	THF	403 (4.29), 425 (4.45), 449 (4.39)	468	904	2.63	0.64	2.4	1.4
	ACN	400 (4.30), 422 (4.47), 445 (4.40)	469	1152	2.41	0.71	2.9	12.0
	solid		537		0.84 (34%) 4.73 (66%)	0.091		
3	hexane	470 (4.63), 500 (4.73)	514	548	3.45	0.74	2.1	10.4
	toluene	478 (4.51), 505 (4.60)	551	1653	3.32	0.66	2.0	10.2
	$CHCl_3$	510 (4.60)	605	3079	2.92	0.30	1.0	23.9
	THF	498 (4.59)	605	3551	1.36	0.14	1.0	63.2
	ACN	495 (4.60)	N.D.[b]	N.D.[b]	N.D.[b]	N.D.[b]		
	solid		624		0.08 (76%) 1.36 (24%)	0.018		
4	hexane	414 (4.28), 436 (4.49), 464 (4.46)	472	365	1.72	0.50	2.9	29.0
	toluene	417 (4.24), 439 (4.44), 466 (4.40)	484	798	2.45	0.65	2.7	26.5
	$CHCl_3$	417 (4.28), 439 (4.48), 466 (4.43)	482	713	2.5	0.78	3.1	8.8
	THF	411 (4.25), 435 (4.44), 459 (4.38)	485	1168	2.51	0.34	1.4	13.5
	ACN	411 (4.31), 431 (4.48), 455 (4.41)	485	1360	2.77	0.52	1.9	18.8
	solid		523		0.58 (41%) 2.28 (59%)	0.22		
5	hexane	484 (4.62), 517 (4.71)	529	439	4.21	0.89	2.1	2.6
	toluene	495 (4.59), 522 (4.64)	571	1644	3.96	0.76	1.9	6.1
	$CHCl_3$	525 (4.63)	617	2840	2.44	0.10	0.4	36.8
	THF	509 (4.57)	620	3517	2.40	0.05	0.5	39.6
	ACN	508 (4.64)	N.D.[b]	N.D.[b]	N.D.[b]	N.D.[b]		
	solid		620		0.08 (46%)	0.093		

					1.31 (54%)			

[a] Molar extinction coefficient at the λ_{abs}.
[b] N.D. = not detected.

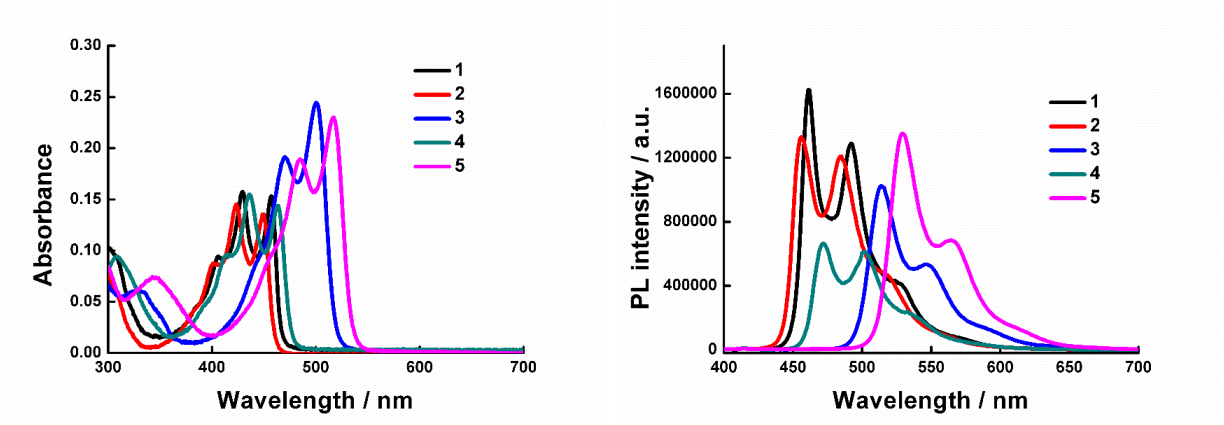

Fig. S2 Absorption and emission spectra of **1-5** in hexanes.

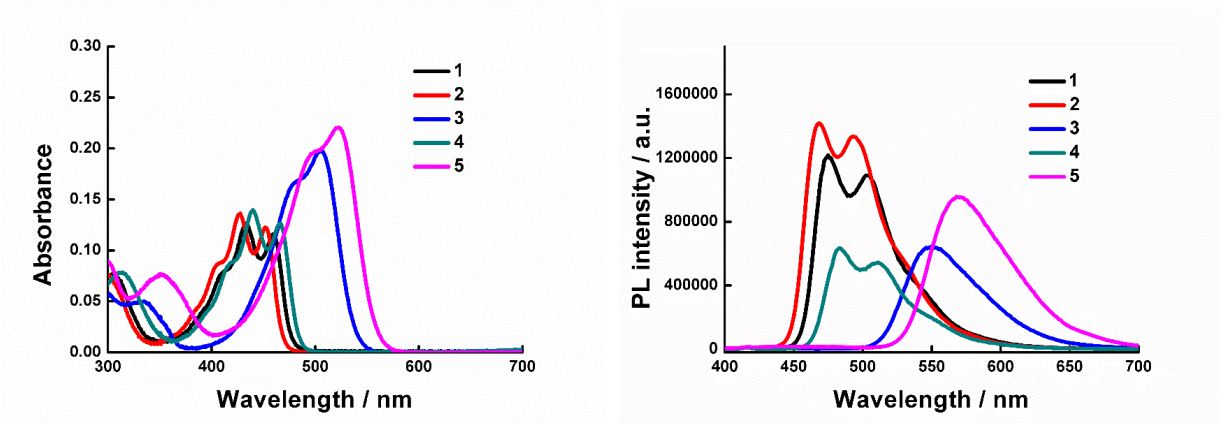

Fig. S3 Absorption and emission spectra of **1-5** in toluene.

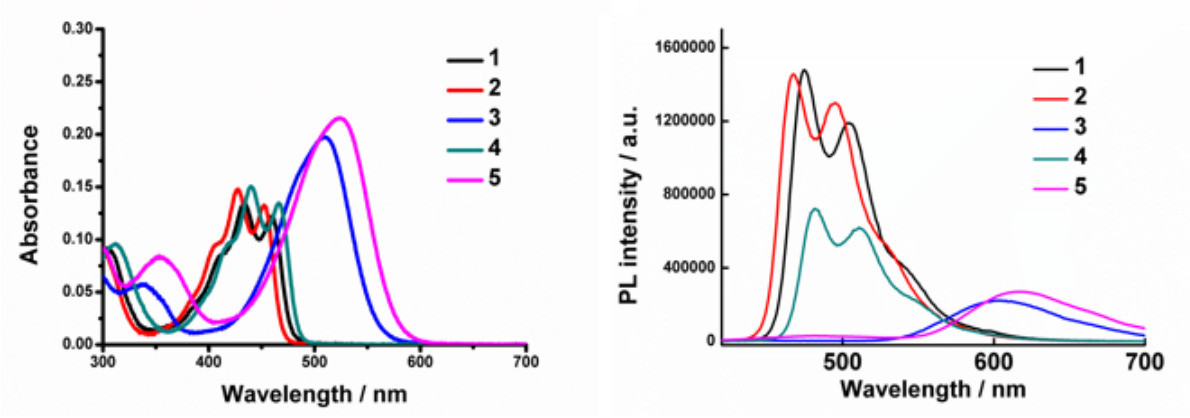

Fig. S4 Absorption and emission spectra of **1-5** in $CHCl_3$.

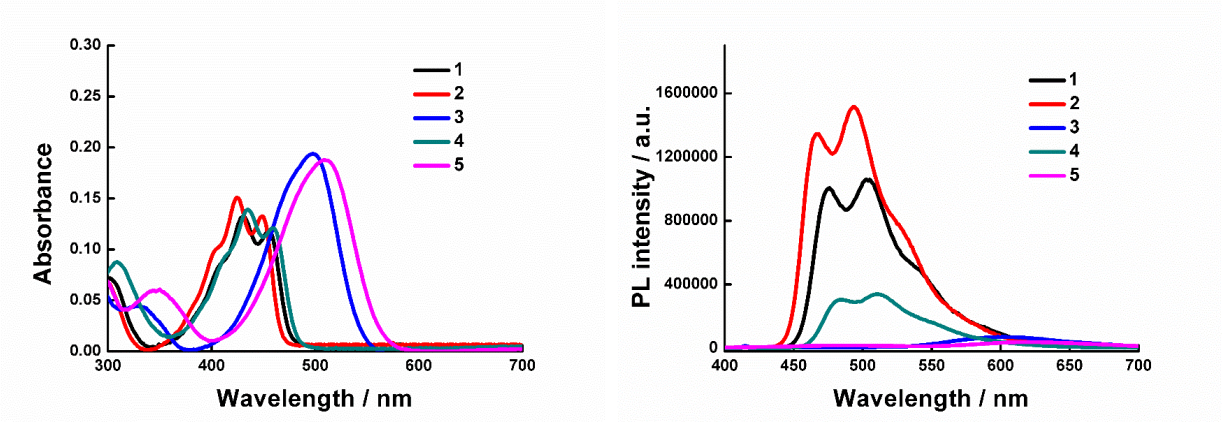

Fig. S5 Absorption and emission spectra of **1-5** in THF

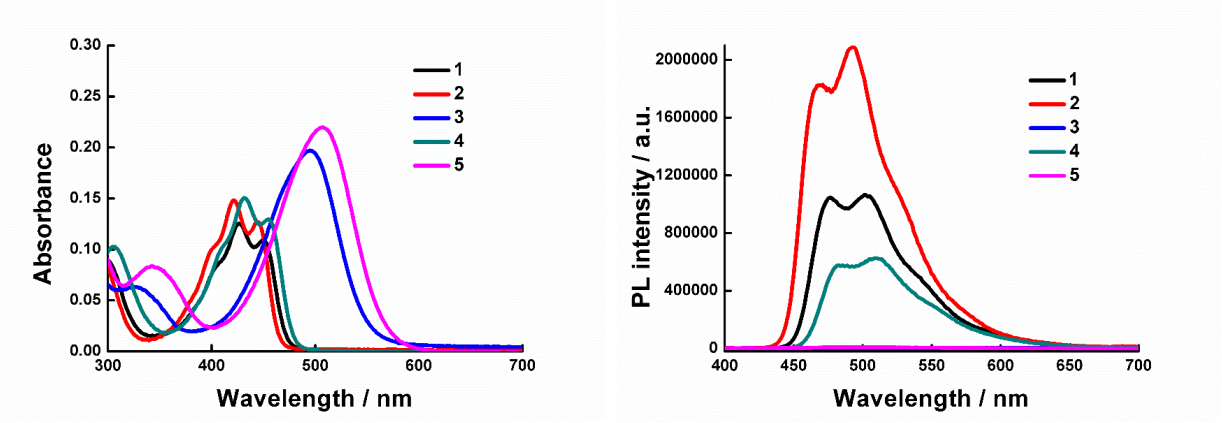

Fig. S6 Absorption and emission spectra of **1-5** in CH_3CN

Table S3. A summary of the dihedral angles, C-H···N, C-H···O, C-H···F and π–π interactions in crystals **1-5**

No.	Dihedral angles (°)	Interaction	Distance (Å)	Angle (°)	Φ (%)[c]
1	*Column A* 4.18 [a] (plane:N1C3C2C1O1B1 and plane:C11-16) *Column B* 3.57 [a] (plane:N3C19C18C17O2B2 and plane:C27-32)	*Column A* F-π (F1-centroid: C5N2 C4C3N1C10) (lone pair to N-ring, D-A) CH/F (F2-C2) CH/F (F2-C12) CH/F (F2-C2) CH/F (C8-F1) π–π (centroid:B1N1C3C2C1O1 to centroid B1N1C3C2C1O1) *Column B* CH/N (N4-C20) CH/F (F4-C22) CH/F (F3-C29) π–π (centroid:C27-32 to centroid:C21N4C20C19N3C26) Between *Column A* and *Column B* CH/F (C15-F3) CH/F (C14-F4)	2.856 3.263 3.403 3.240 3.324 3.885 3.392 3.359 3.418 3.588 3.410 3.545	131.93 146.30 160.80 124.68 138.46 138.66 159.80 155.17 166.00 153.30	2.01
2	5.37 [a] (plane:N14C3C4C5O2B1 and plane:C16-21)	CH/F (F2-C11) CH/F (F2-C15) CH/N (C15-N7) CH/F (F1-C15) π–π (centroid:C16-21 to centroid:C13N14C5C6N7C8)	3.153 3.304 3.578 3.473 3.620	119.56 164.88 162.74 152.14	9.13
3	12.06 [a] (plane:C3C4C5N14O2B1 and plane:C16-21)	CH/F (F1-C15) CH/O (O2-C27) π–π (centroid:C16-21 to centroid:C8-13) π–π (centroid:C16-21 to centroid:C5N14C13C8N7C6 π–π (centroid:C5N14C13C8 N7C6 to centroid:C16-21) π–π (centroid:C3C4O2B1N14 C5 to centroid:C3C4O2B1N14 C5	3.453 3.395 3.656 3.698 3.660 3.625	160.90 144.00	1.78

4	12.72 [a] (plane:C11-16 and plane: C1C2C3N1B1O1) 57.89 [b] (plane:C17-22 and plane: C10C5N2C4C3N1)	CH/F (C16-F2) CH/F (F1-C18) CH/F (F1-C20) π–π (centroid: C11-16 to centroid: C10N1C3C4N2C5)	3.398 3.244 3.383 3.649 3.717	145.40 129.10 140.70	22.0
5	22.05 [a] (plane:C13-18 and plane: C10C11C12N1B1O1) 44.14 [b] (plane:C32-C37 and plane C9C10N1C2C7N8)	F-π (F1-centroid:C2-7) CH/N (N8-C21) CH/F (F2-C18) CH/O (O1-C33) CH/F (F1-C24) CH/π (C27-centroid:C13-18) CH/F (F1-C35) π–π (centroid: C9N8C7 C2N1C10 to centroid C13-18) π–π (centroid: C2-7 to centroid: C2-7)	3.871 3.569 3.286 3.460 3.350 3.633 3.197 3.725 3.646	109.50 161.93 131.30 151.48 146.50 126.03 119.42	9.31

[a] The dihedral angle between the quinoxaline-BF_2 core and phenyl/triphenylamino substituent (**R'**).
[b] The dihedral angle between the quinoxaline-BF_2 core and additional phenyl substituent (**R**).
[c] Solid-state fluorescence quantum yields.

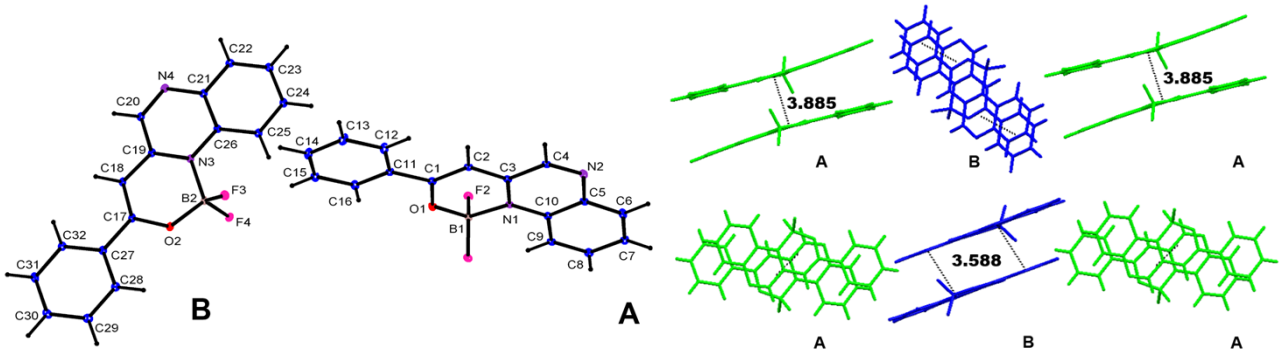

Fig. S7 ORTEP (left) and π−π interactions in the packing diagram (right) of conformational independent structures (A: green, B: blue) identified in the unit cell of **1**.

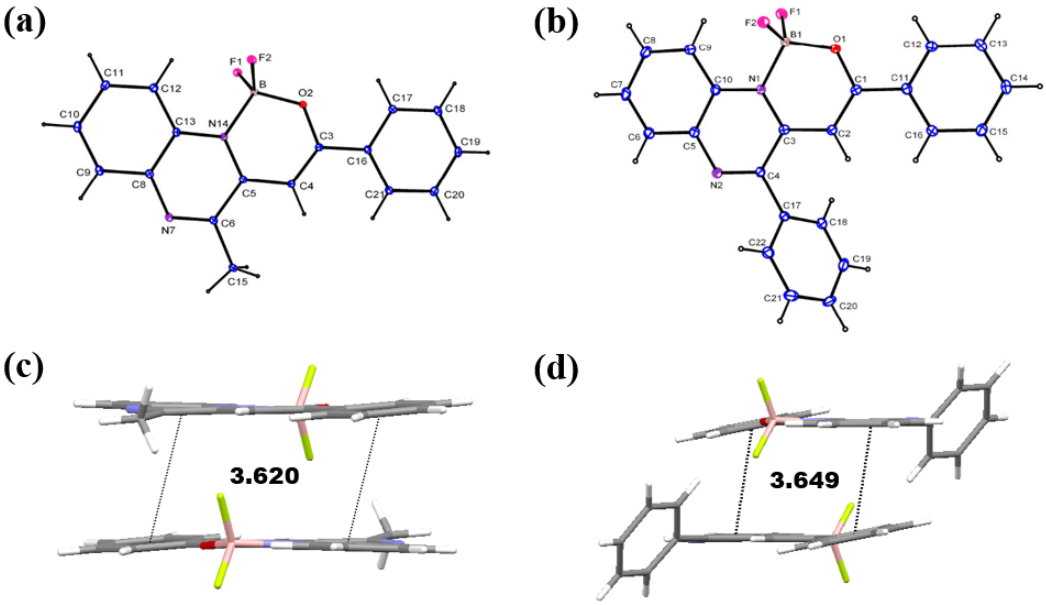

Fig. S8 ORTEP (a, b) and π−π interactions in the packing diagram (c, d) of crystals **2** and **4**.

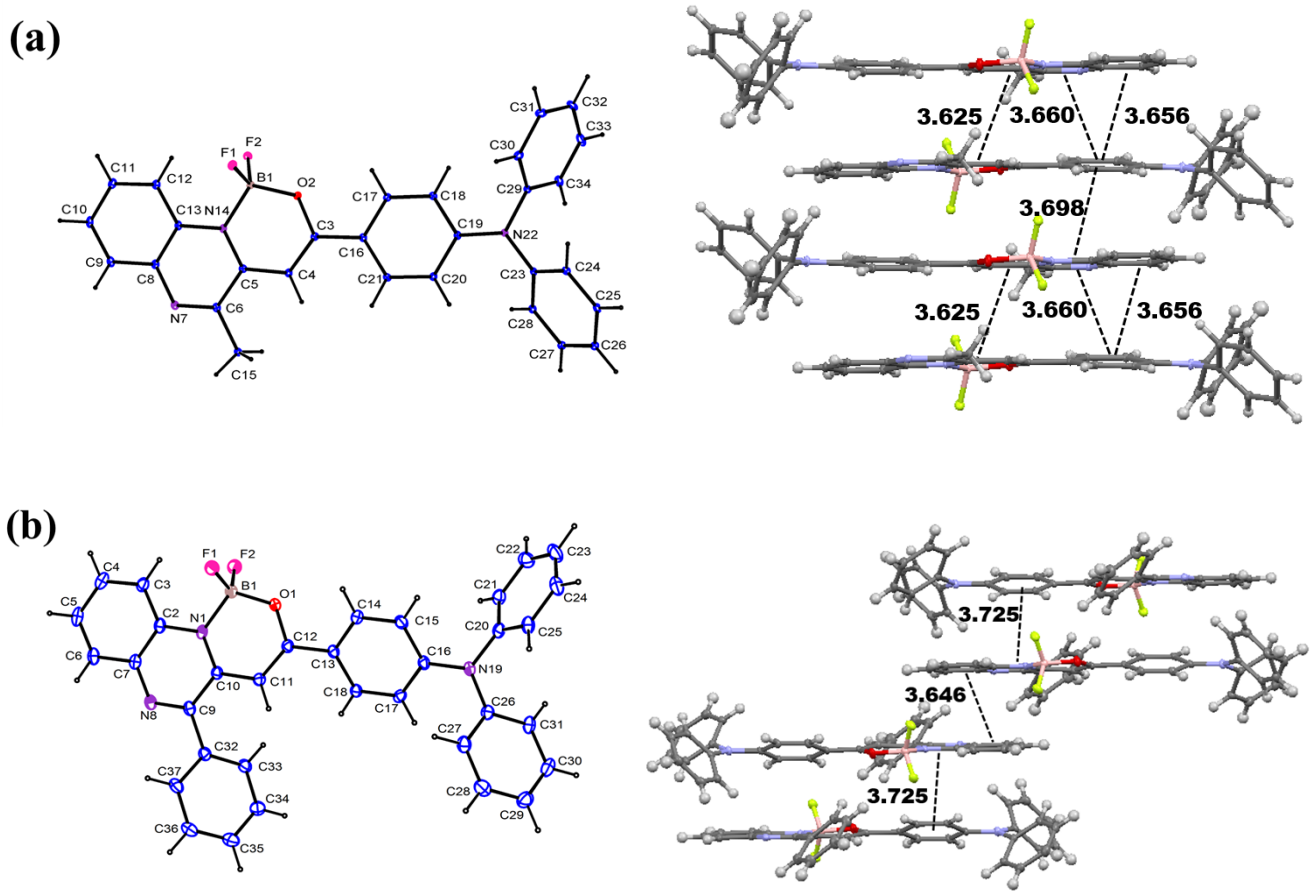

Fig. S9 ORTEP (left) and crystal packing (right) diagrams of **3** (a) and **5** (b)

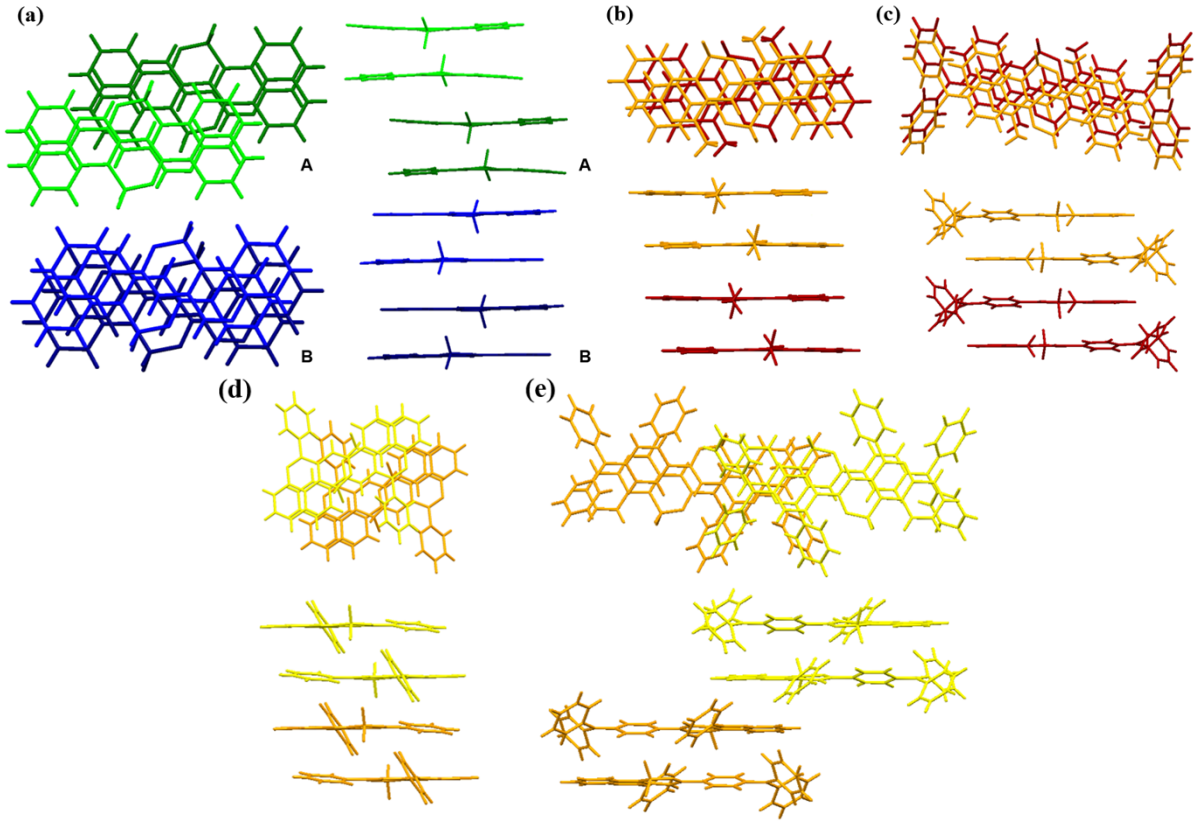

Fig. S10 The overlap between adjacent dimers in packings of (a) **1**; (b) **2**; (c) **3** ; (d) **4** ; (e) **5**.

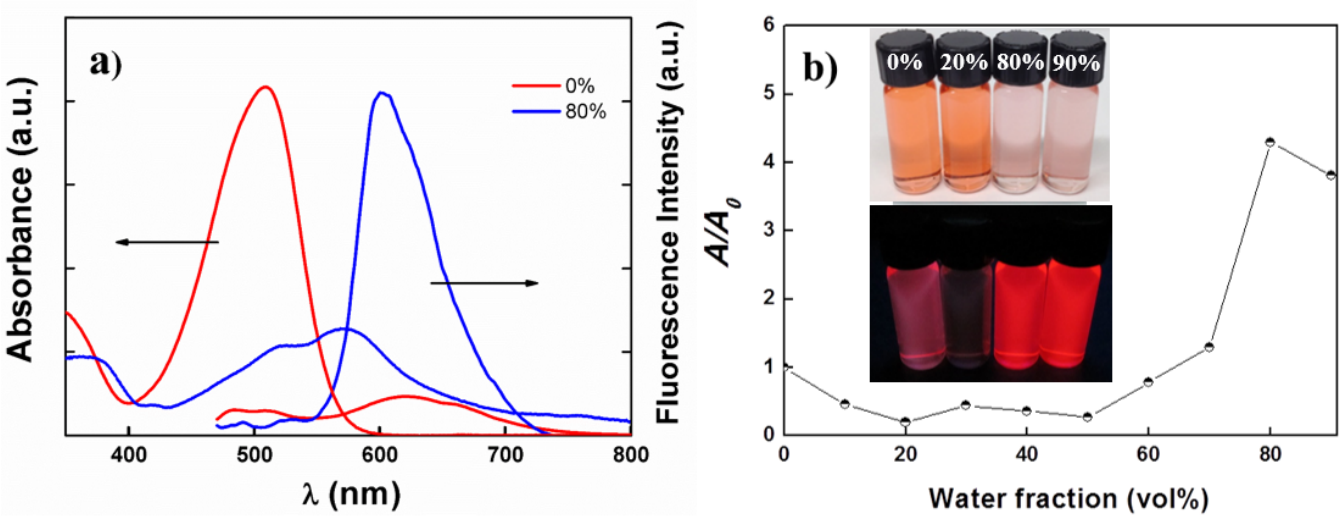

Fig. S11 (a) Absorption and fluorescence spectra (λ_{ex} = 450 nm) of **5** in solution (pure THF, 10^{-6} M) and aggregate state (water/THF = 8/2, v/v); (b) Effect of solvent composition on the fluorescence (where A_0 and A are the integrated areas of the PL peaks in THF and THF/water mixture, respectively). Insert photo: the aqueous mixture taken under naked eye and 365nm UV lamp with different water fractions.

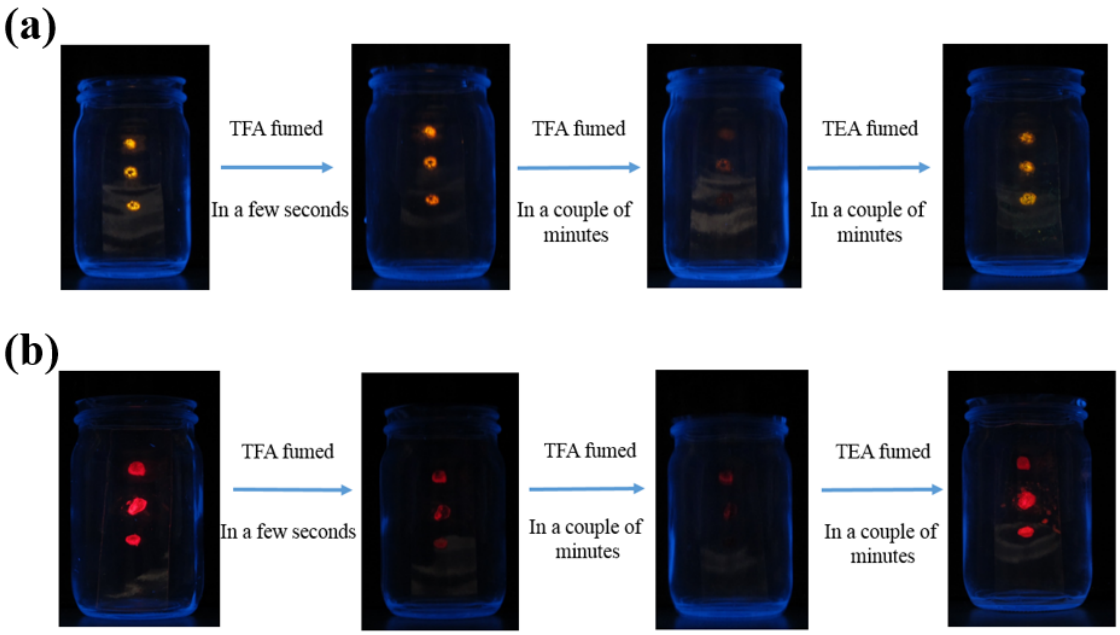

Fig. S12 The fluorescence images of (a) **4** and (b) **5** by treating with TFA and TEA vapor in a closed container.

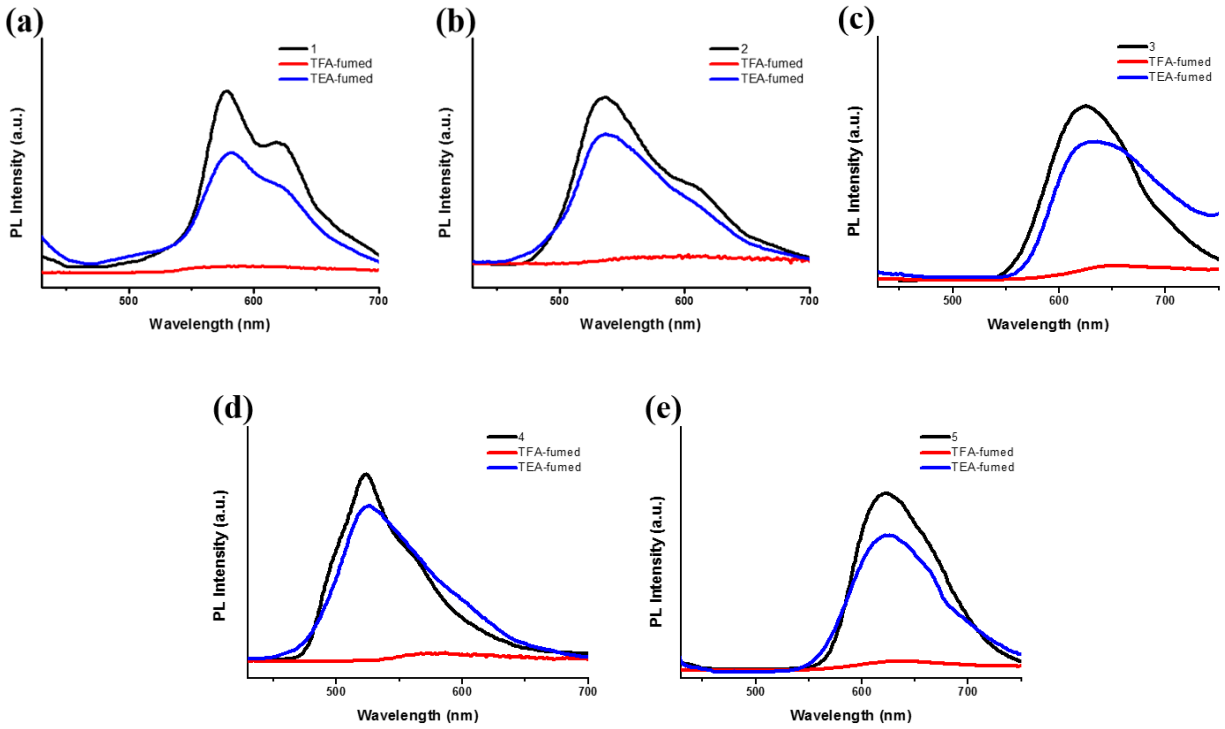

Fig. S13 The solid-state fluorescence spectra of (a) **1**; (b) **2**; (c) **3**; (d) **4**; (e) **5** after TFA-fuming and TEA-fuming.

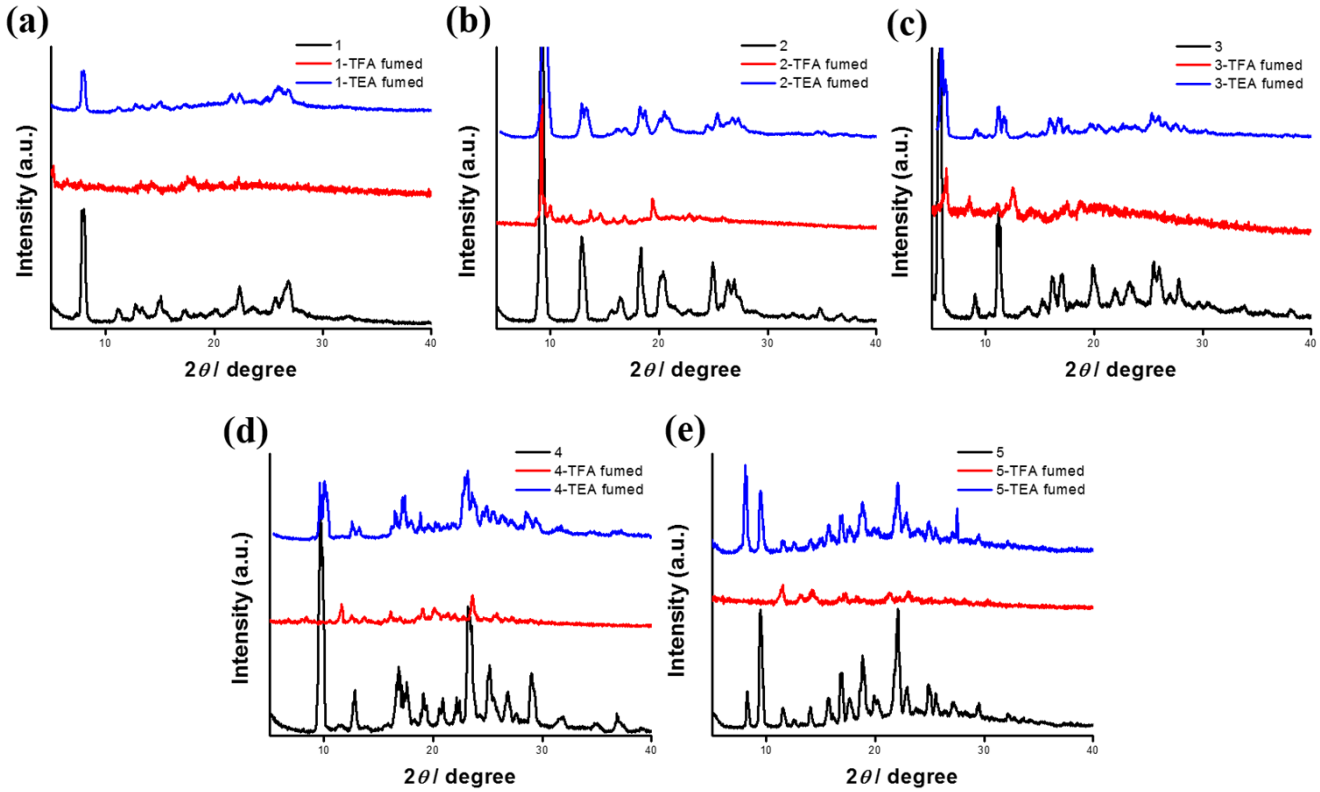

Fig. S14 The comparison of PXRD patterns of (a) **1**; (b) **2**; (c) **3**; (d) **4**; (e) **5** after TFA-fuming and TEA-fuming.

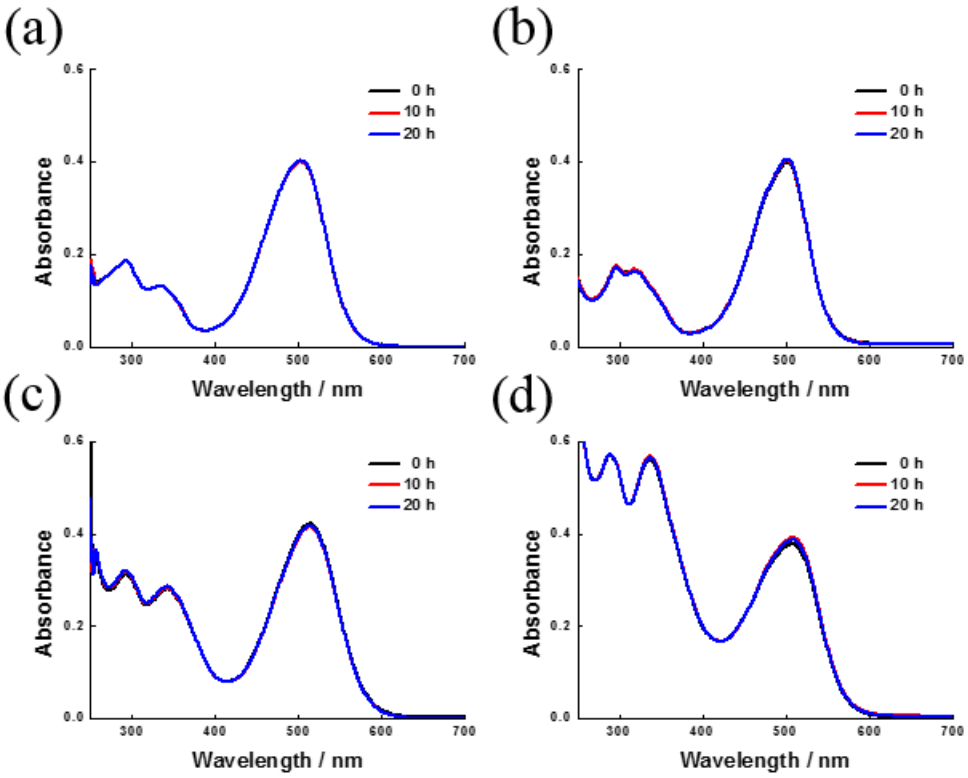

Fig. S15 The stability test of absorption spectra of **3** (up) and **5** (down) in DMSO (a, c) and EtOH (b, d).

Table S4. Crystal data and structure refinements for **1-5**

CCDC number	953115	953117	953118	966717	966718
Identification code	**1**	**2**	**3**	**4**	**5**
Empirical formula	C32H22B2F4N4O2	C17H13BF2N2O	C29H22BF2N3O	C22H15BF2N2O	C34H24BF2N3O
Formula weight	592.16	310.10	477.31	372.17	539.37
Temperature, K	100.0(1)	100.0(1)	100.0(1)	100.0(1)	100.0(1)
Wavelength, Å	0.71073	0.71073	0.71073	0.71073	0.71073
Crystal system	Triclinic	Triclinic	Monoclinic	Triclinic	Monoclinic
Space group	P-1	P-1	P2(1)/n	P-1	P2(1)/n
a, Å	6.9566(4)	7.0915(3)	18.0013(6)	7.1054(7)	14.9332(5)
b, Å	8.3315(5)	10.1014(5)	6.9212(2)	11.1114(10)	11.3243(4)
c, Å	23.1202(12)	10.3857(5)	20.2630(7)	11.9627(12)	17.9422(6)
α, deg	95.844(2)	86.948(2)	90	96.493(3)	90
β, deg	90.570(2)	70.9880(10)	116.034(2)	106.301(3)	94.526(2)
γ, deg	96.433(2)	86.6970(10)	90	105.521(2)	90
Volume, $Å^3$	1324.35(13)	701.75(6)	2268.42(13)	855.17(14)	3024.71(18)
Z	2	2	4	2	4
Density (calcd), Mg/m^3	1.485	1.468	1.398	1.445	1.184
Absorption coefficient, mm^{-1}	0.112	0.110	0.097	0.104	0.080
F(000)	608	320	992	384	1120
Theta range for data collection	0.89 to 26.37°.	2.02 to 26.37°	1.26 to 26.37°	1.81 to 27.10°	1.71 to 26.37°
Index ranges	-8<=h<=8, -10<=k<=10,	-8<=h<=8, -12<=k<=12,	-22<=h<=22, -8<=k<=8,	-8<=h<=9, -14<=k<=14,	-18<=h<=18, -14<=k<=14,

	-28<=l<=28	-12<=l<=12	-25<=l<=25	-15<=l<=15	-22<=l<=22
Reflections collected	20395	10745	35985	13395	45985
Independent reflections	5429 [R(int) = 0.0281]	2862 [R(int) = 0.0269]	4648 [R(int) = 0.0621]	3761 [R(int) = 0.0268]	6196 [R(int) = 0.0823]
Max. and min. transmission	0.9888 and 0.9692	0.989 and 0.9674	0.9885 and 0.9716	0.9877 and 0.9695	0.992 and 0.9701
Data / restraints / parameters	5429 / 124 / 398	2862 / 65 / 210	4648 / 101 / 327	3761 / 0 / 253	6196 / 115 / 370
Goodness-of-fit on F^2	1.022	1.017	1.010	1.042	1.129
R1, wR2 [I>2sigma(I)]	0.0351, 0.0798	0.0353, 0.0855	0.0401, 0.0857	0.0513, 0.1463	0.0631, 0.1579
R1, wR2 (all data)	0.0510, 0.0886	0.0516, 0.0956	0.0727, 0.1025	0.0627, 0.1579	0.1192, 0.1740
Largest diff. peak and hole	0.278 and -0.195 e.Å^{-3}	0.260 and -0.198 e.Å^{-3}	0.236 and -0.208 e.Å^{-3}	0.728 and -0.276 e.Å^{-3}	0.232 and -0.216 e.Å^{-3}

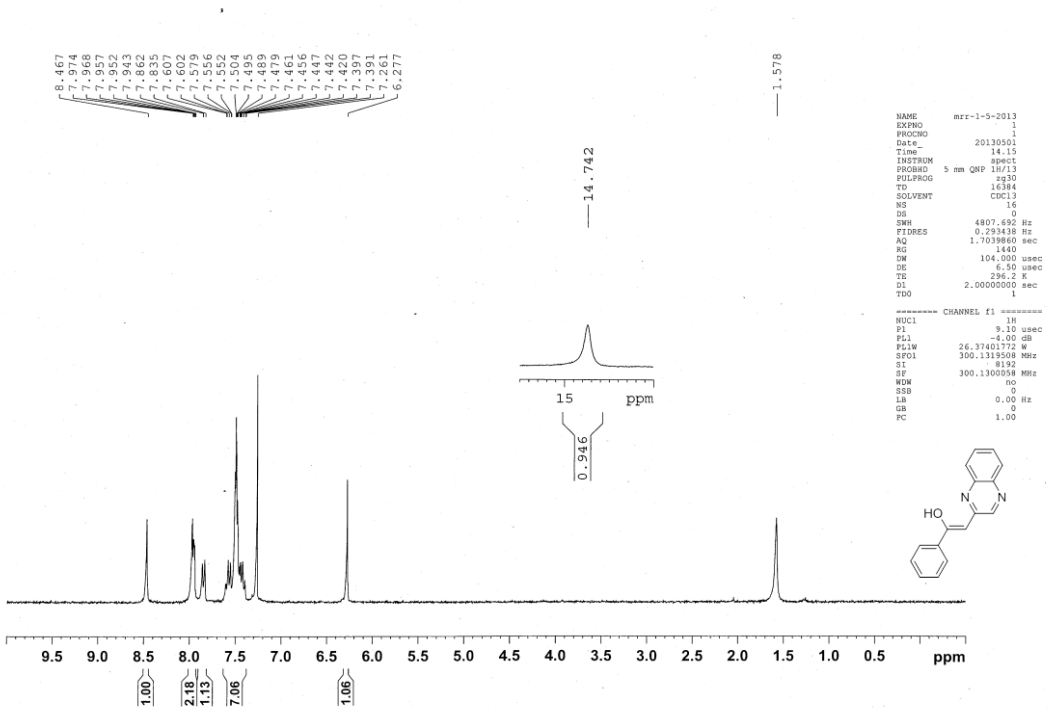

Fig. S16 ^{1}H NMR spectrum of **1a** in $CDCl_3$

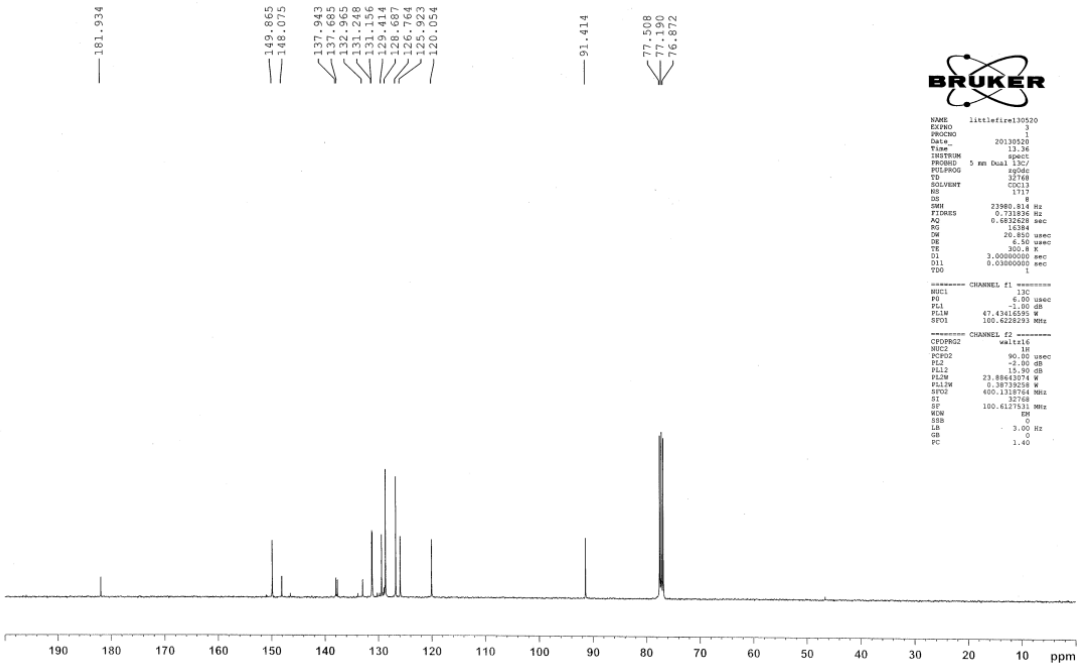

Fig. S17 ^{13}C NMR spectrum of **1a** in $CDCl_3$

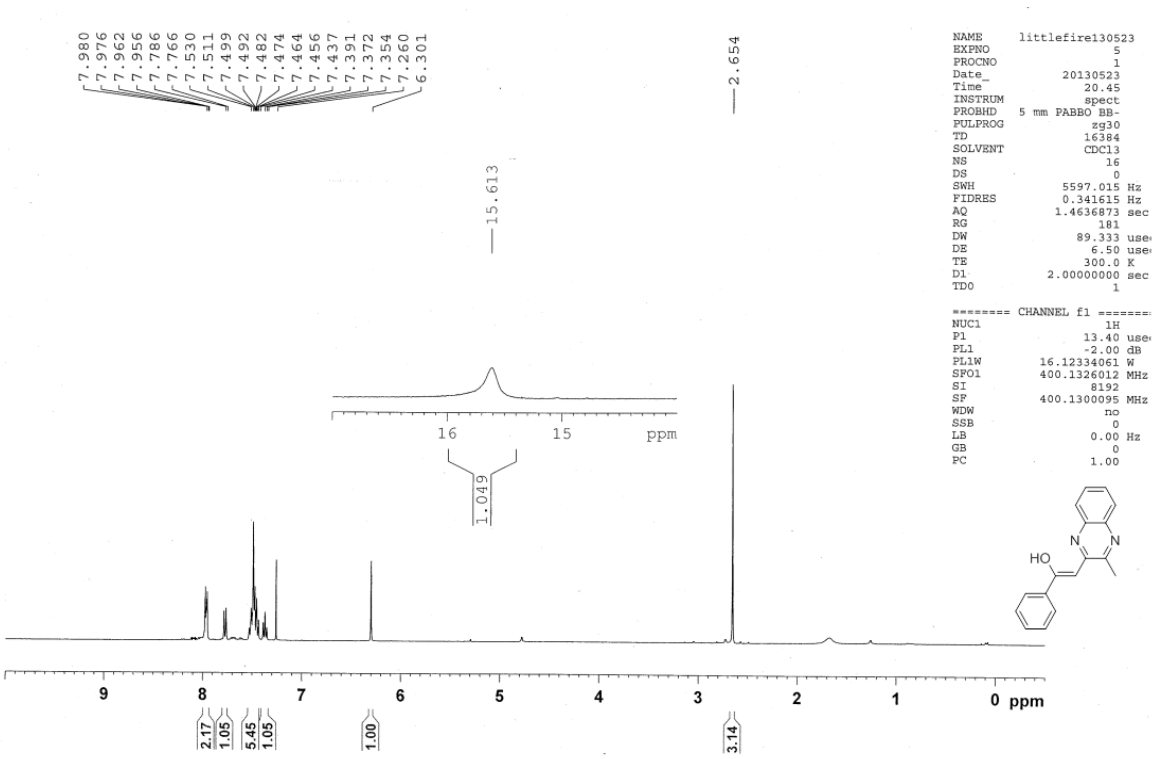

Fig. S18 ^{1}H NMR spectrum of **2a** in $CDCl_3$

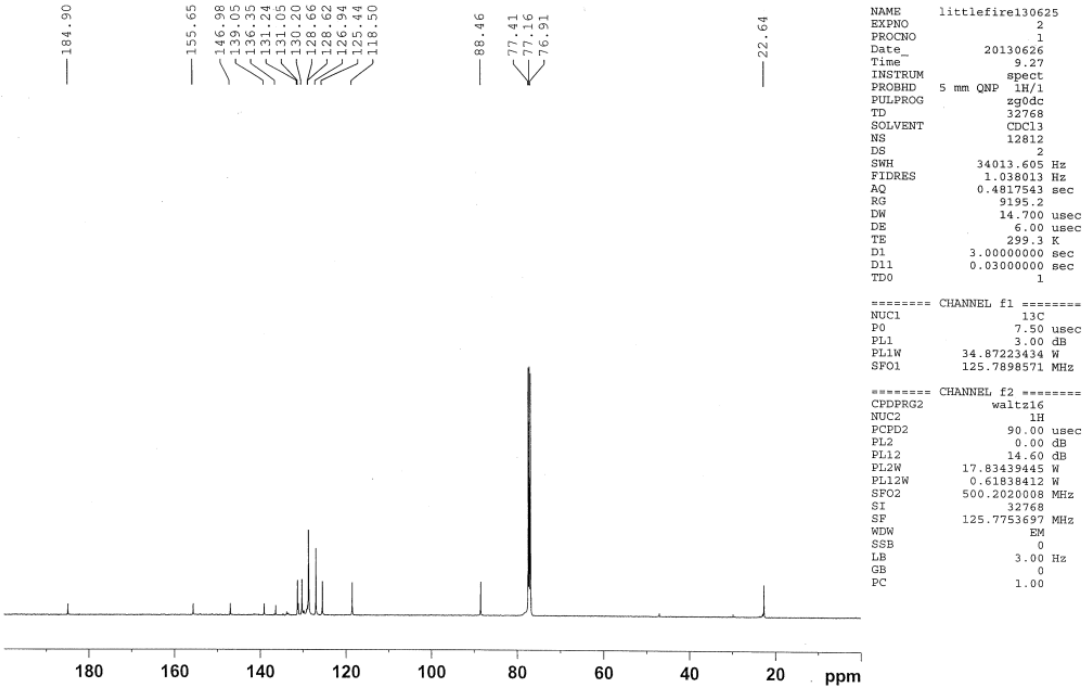

Fig. S19 ^{13}C NMR spectrum of **2a** in $CDCl_3$

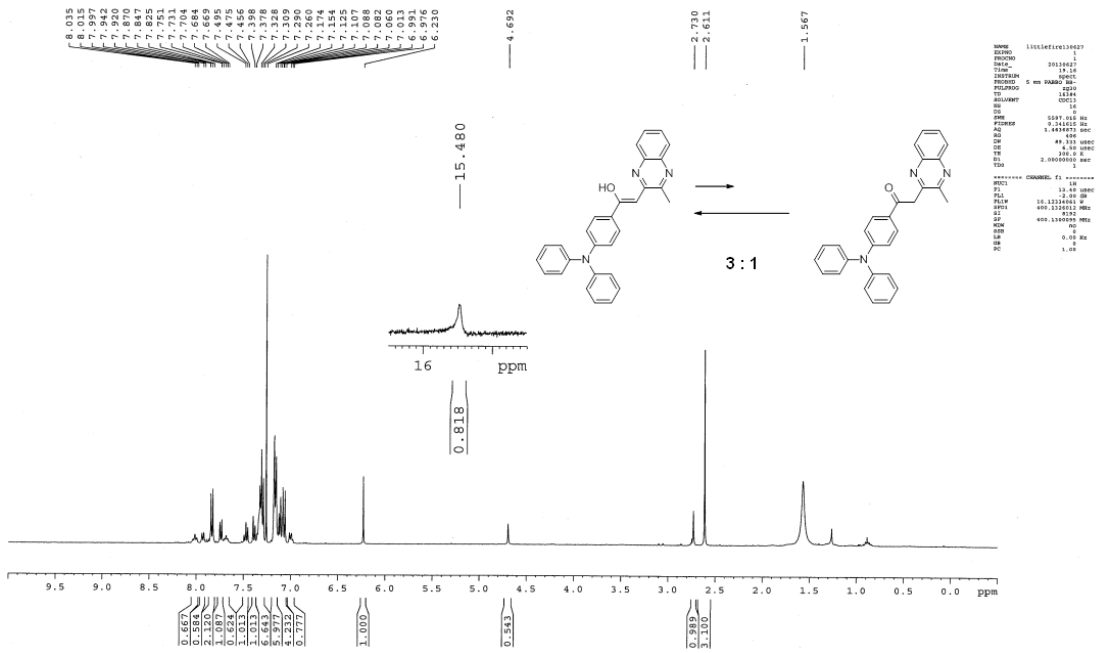

Fig. S20 ^{1}H NMR spectrum of **3a** in $CDCl_3$

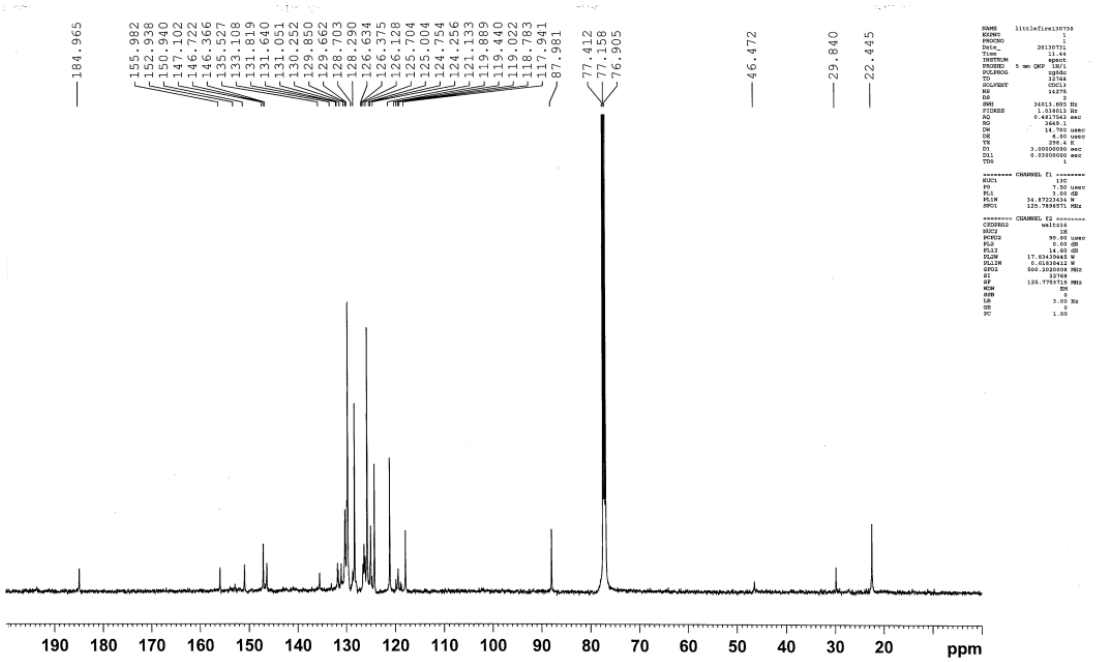

Fig. S21 ^{13}C NMR spectrum of **3a** in $CDCl_3$

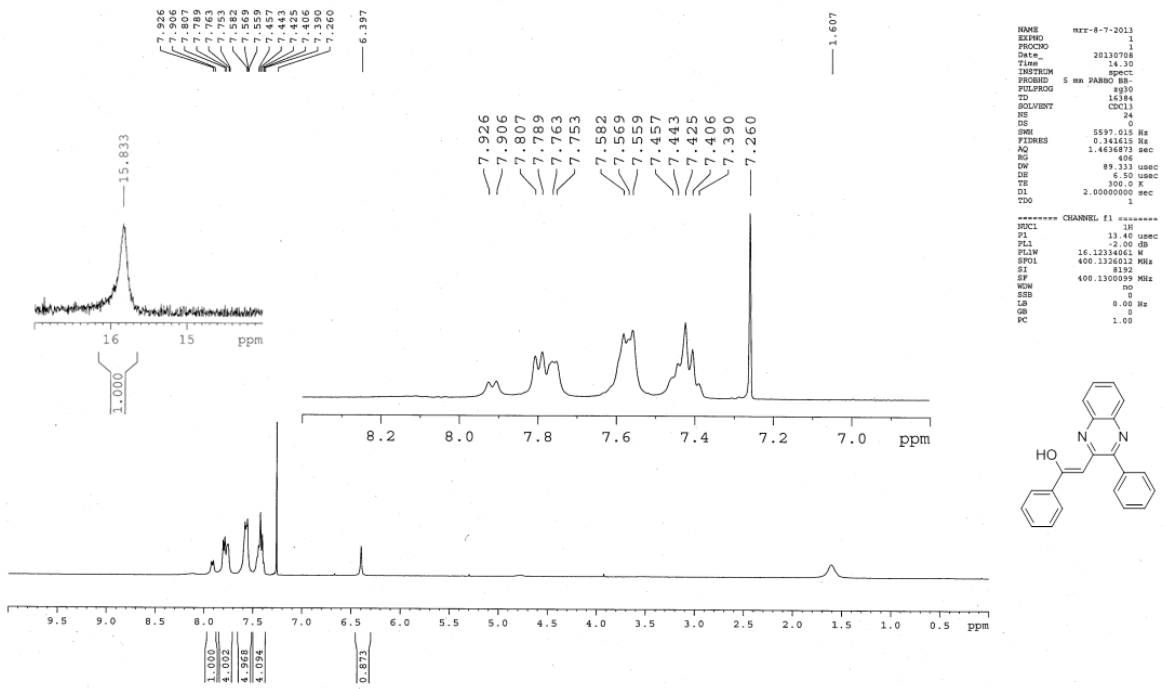

Fig. S22 ^{1}H NMR spectrum of **4a** in $CDCl_3$

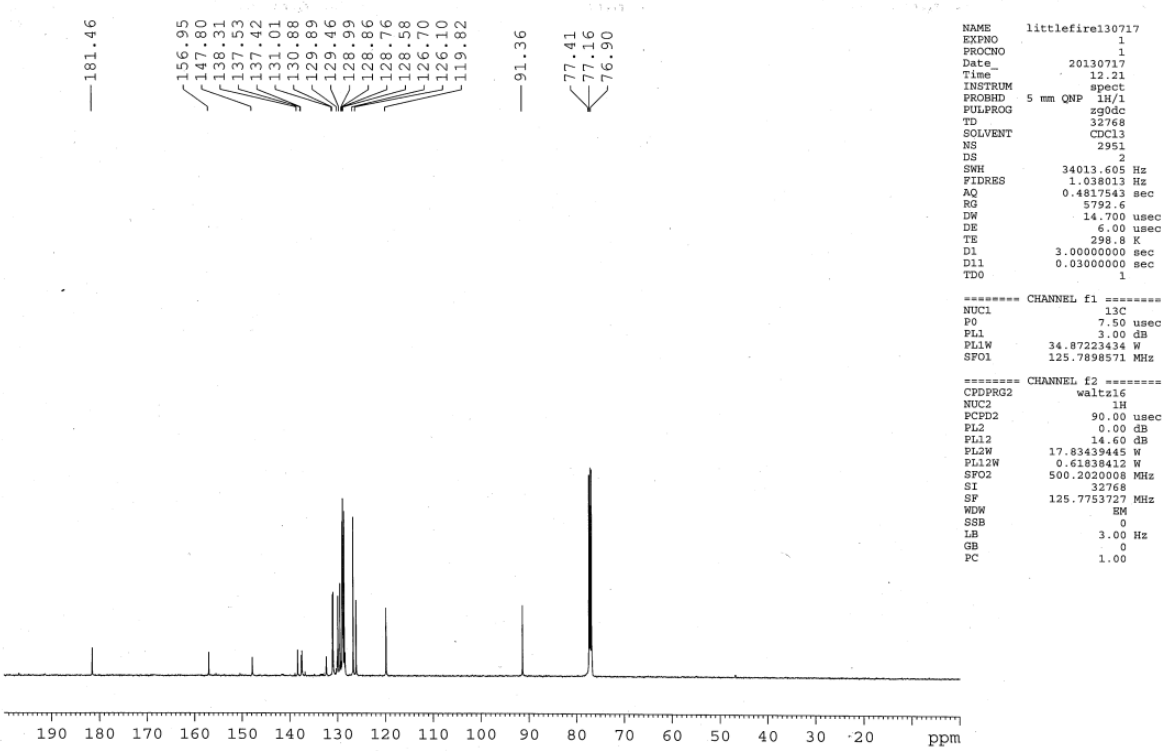

Fig. S23 ^{13}C NMR spectrum of **4a** in $CDCl_3$

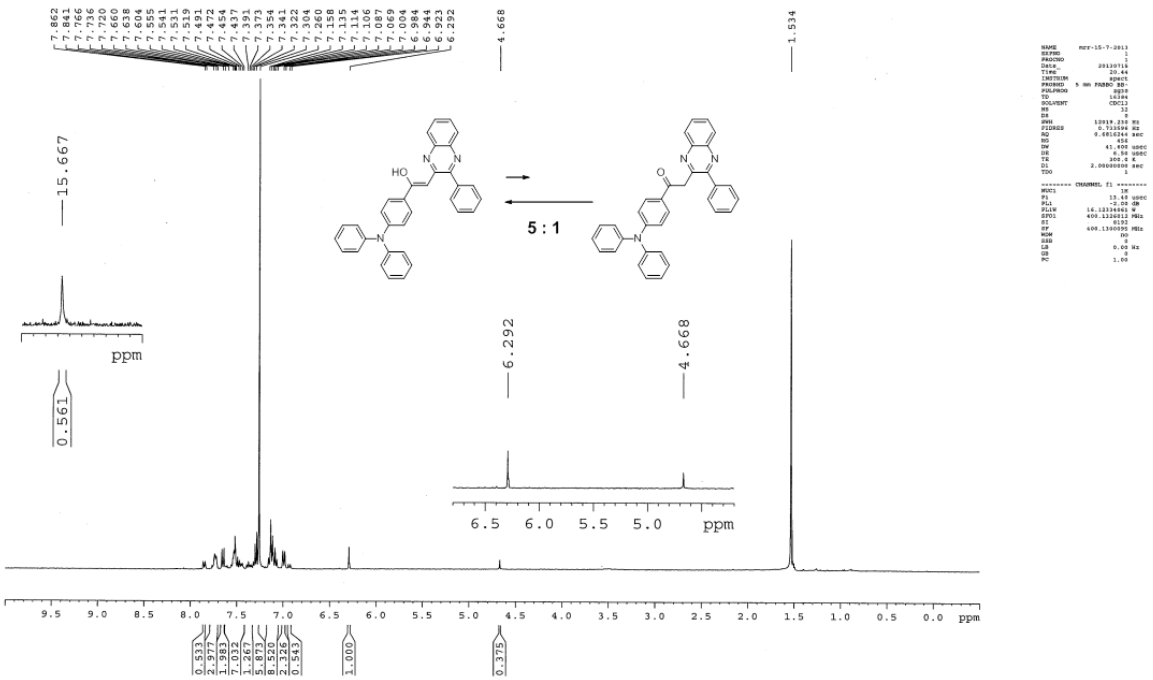

Fig. S24 ^{1}H NMR spectrum of **5a** in $CDCl_3$

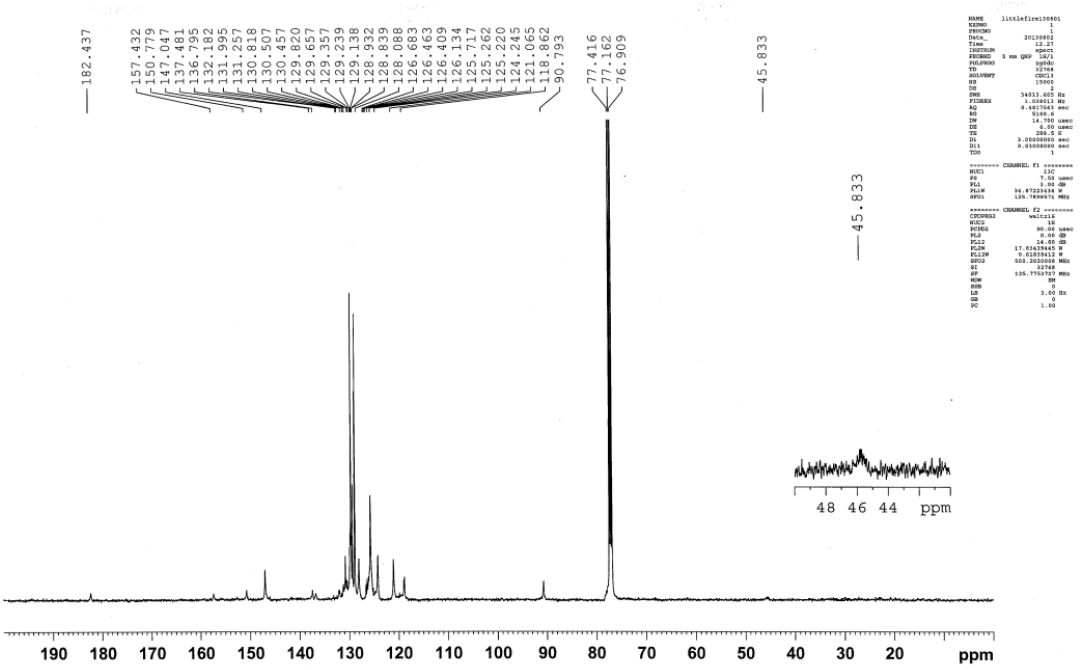

Fig. S25 ^{13}HC NMR spectrum of **5a** in $CDCl_3$

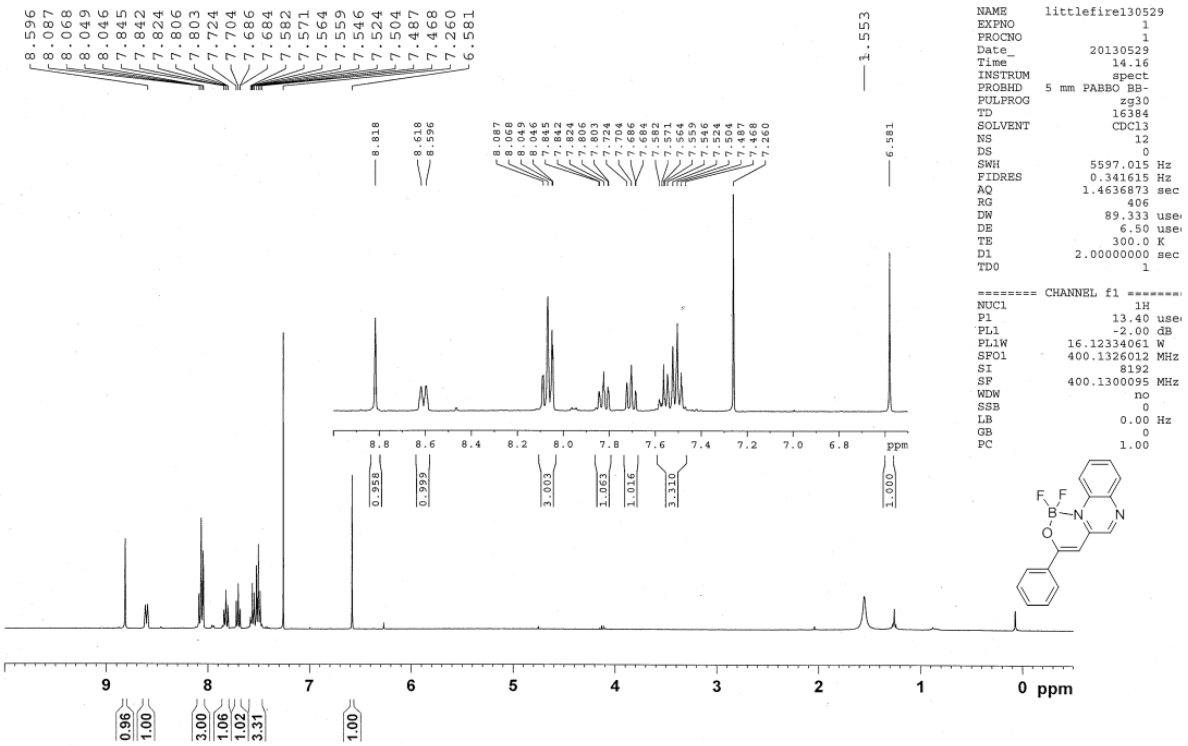

Fig. S26 ^{1}H NMR spectrum of **1** in $CDCl_3$

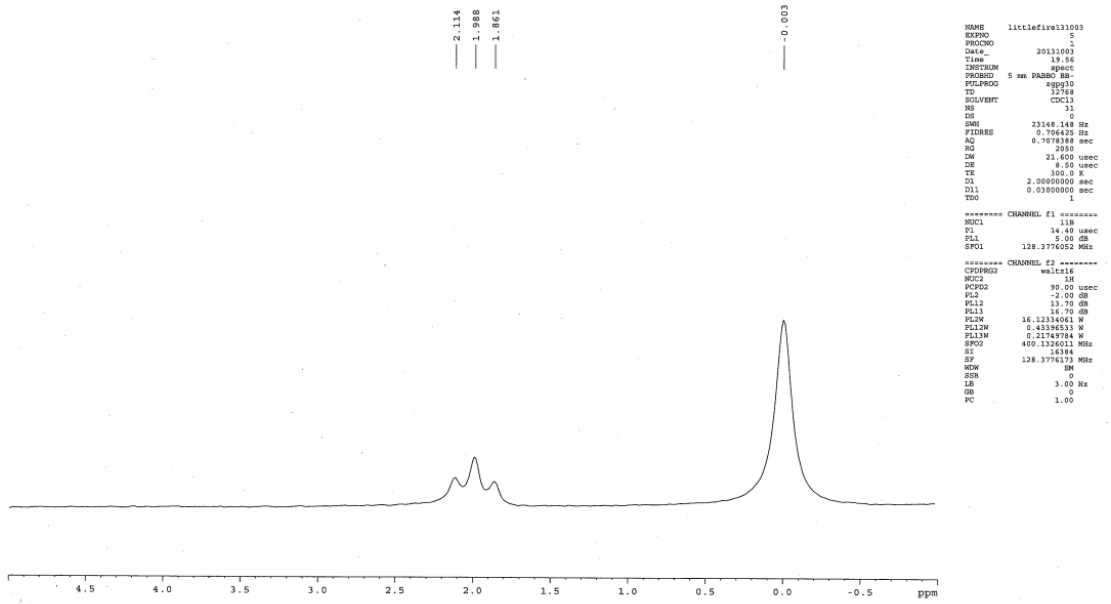

Fig. S27 ^{11}B NMR spectrum of **1** in $CDCl_3$

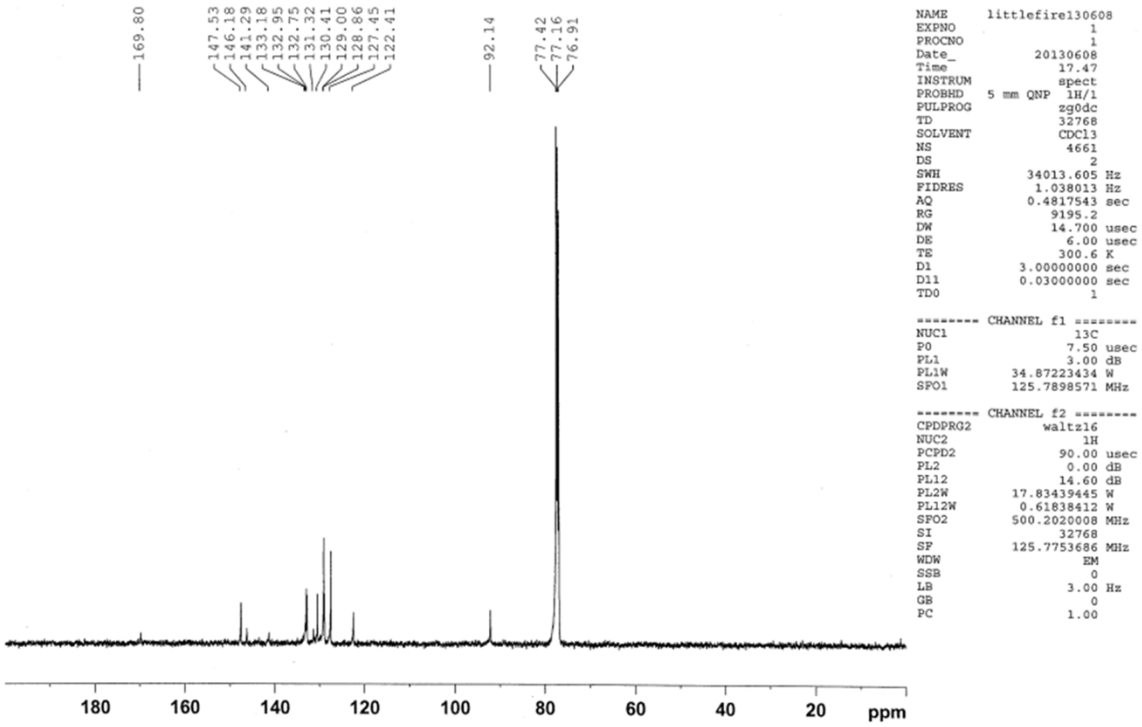

Fig. S28 ^{13}C NMR spectrum of **1** in $CDCl_3$

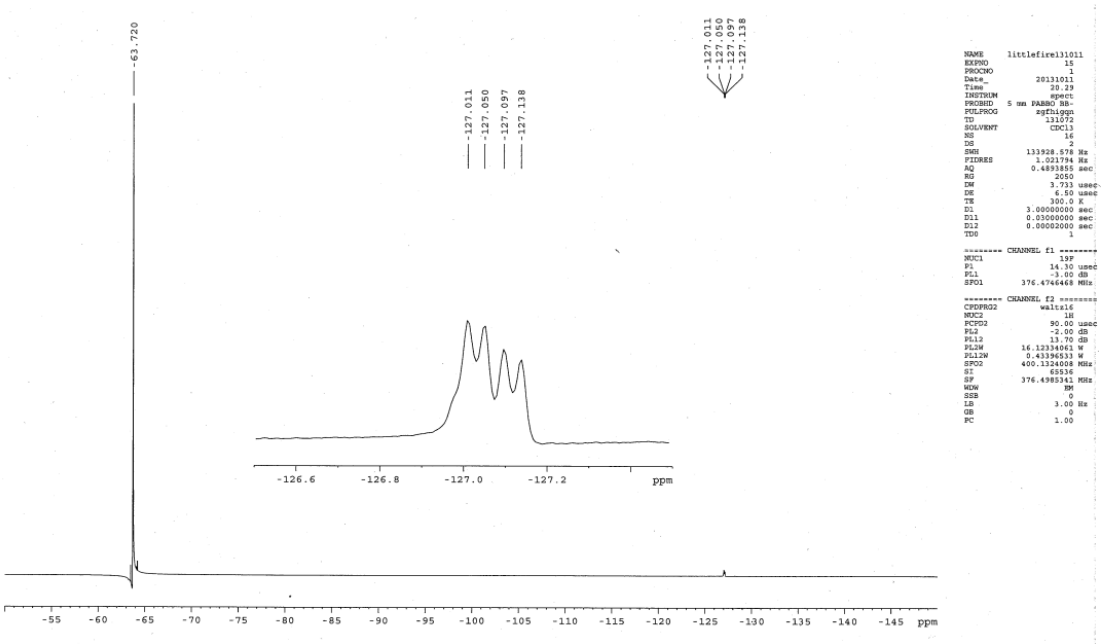

Fig. S29 ^{19}F NMR spectrum of **1** in $CDCl_3$

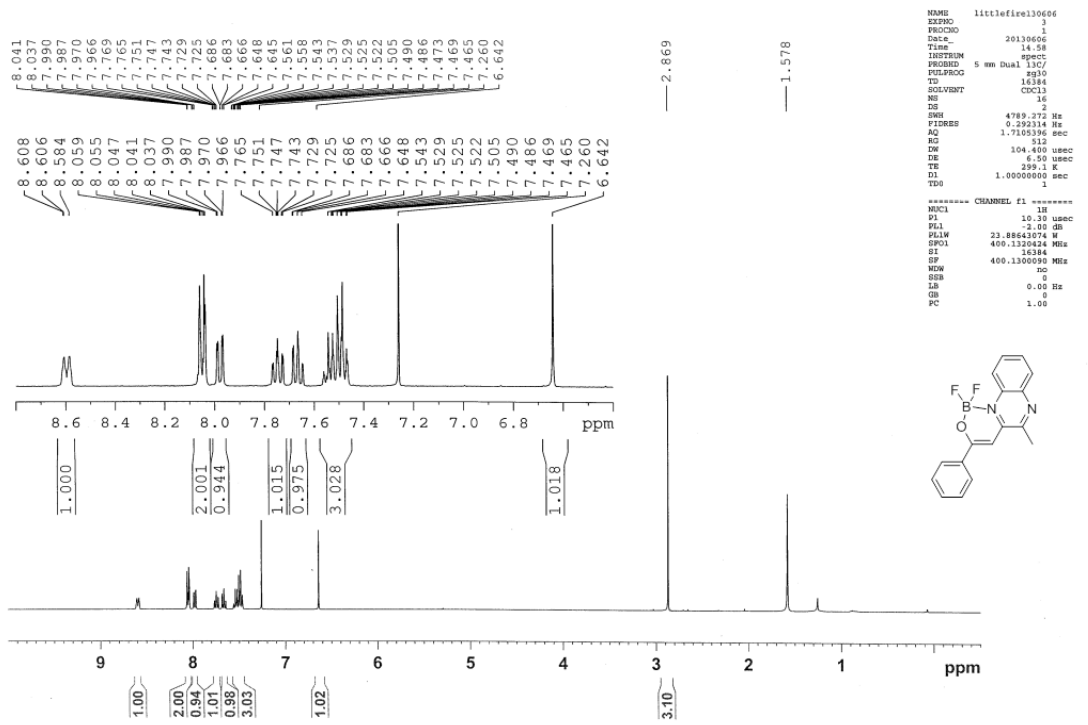

Fig. S30 ^{1}H NMR spectrum of **2** in $CDCl_3$

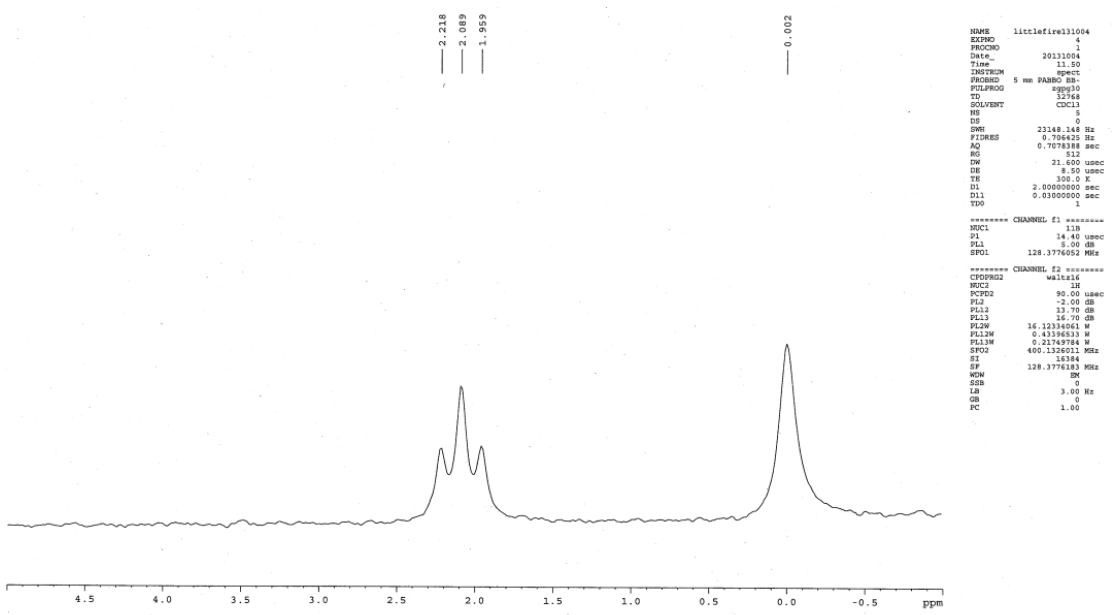

Fig. S31 ^{11}B NMR spectrum of **2** in $CDCl_3$

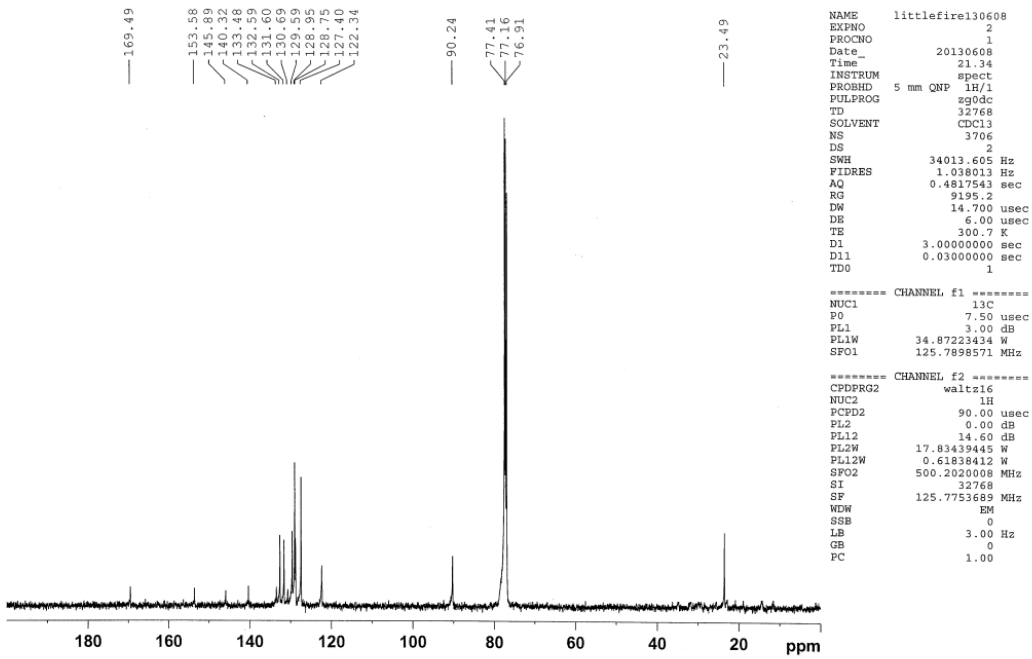

Fig. S32 ^{13}C NMR spectrum of **2** in $CDCl_3$

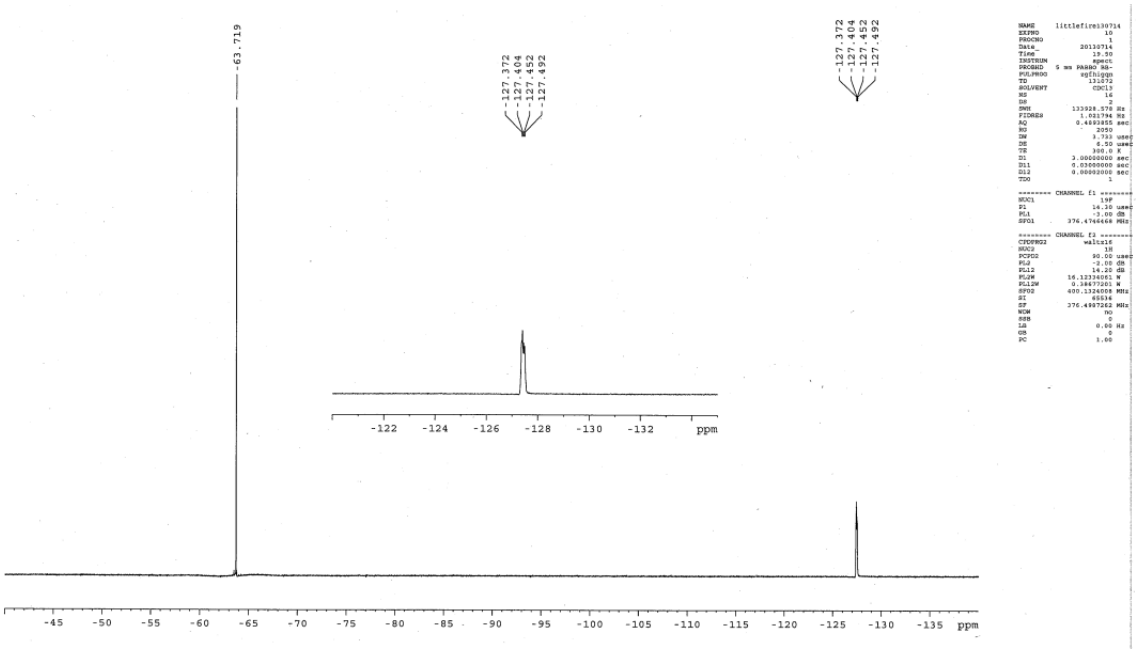

Fig. S33 ^{19}F NMR spectrum of **2** in $CDCl_3$

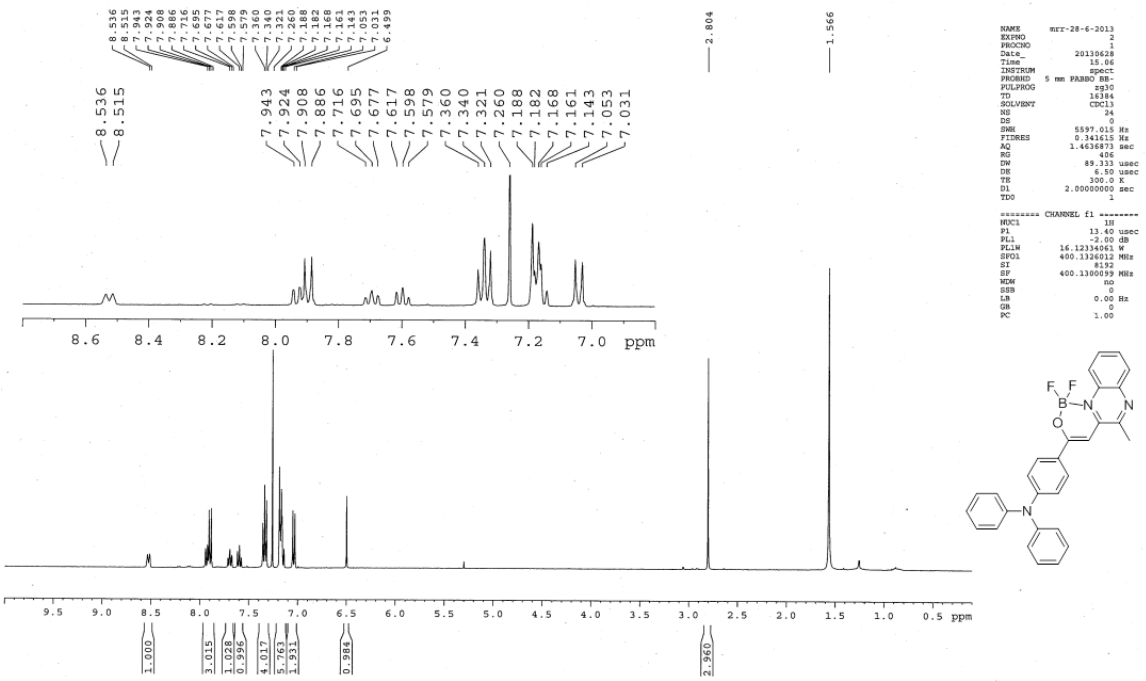

Fig. S34 ^{1}H NMR spectrum of **3** in $CDCl_3$

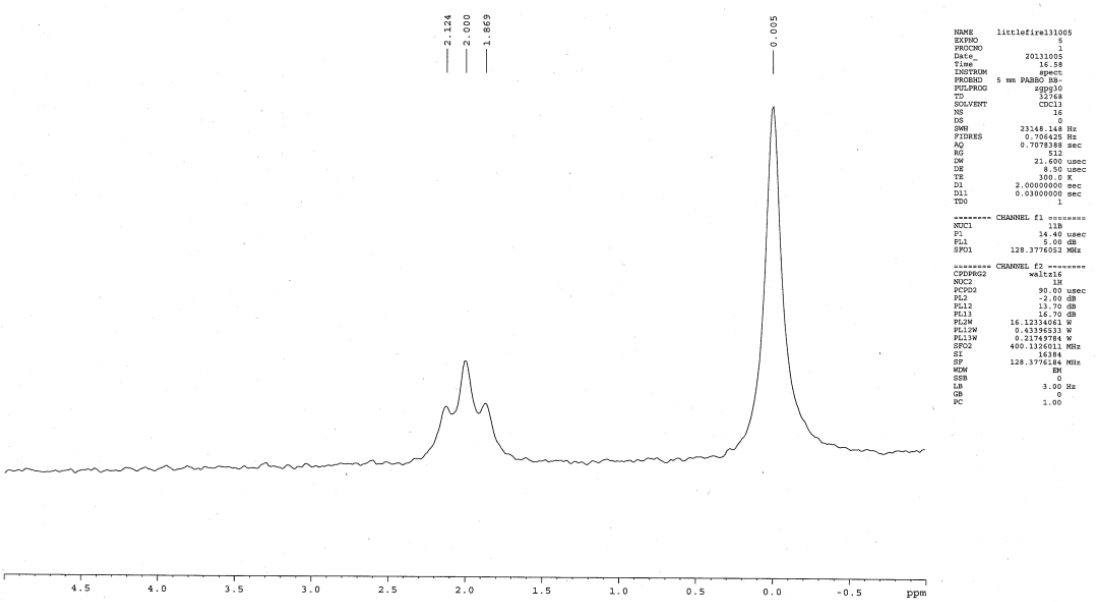

Fig. S35 ^{11}B NMR spectrum of **3** in $CDCl_3$

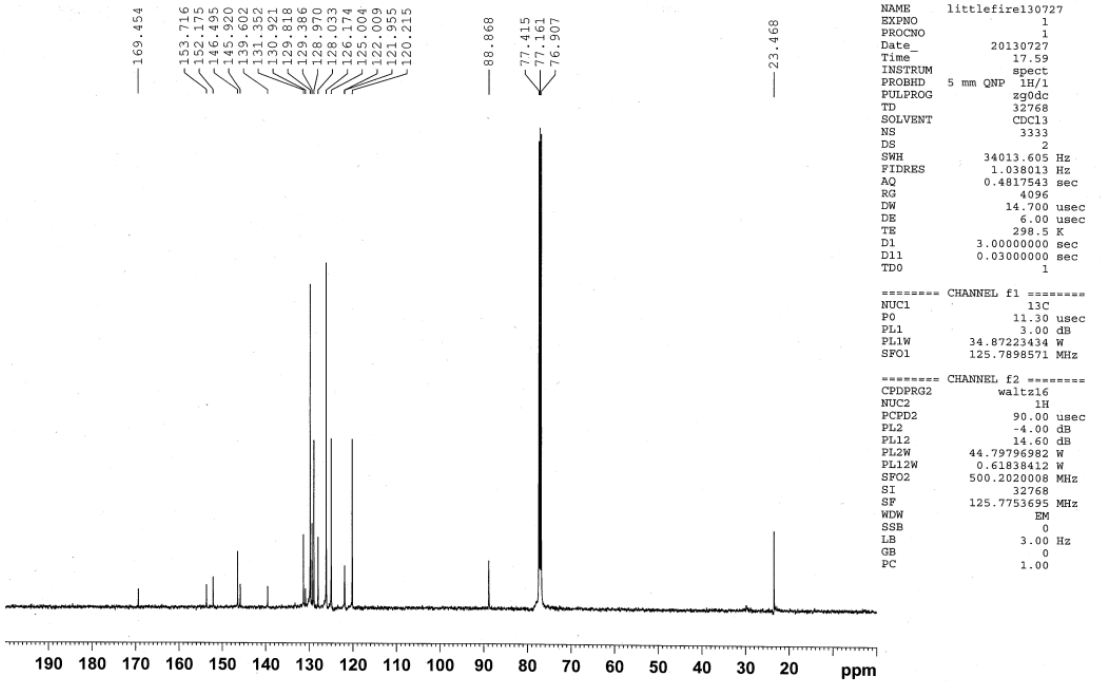

Fig. S36 ^{13}C NMR spectrum of **3** in $CDCl_3$

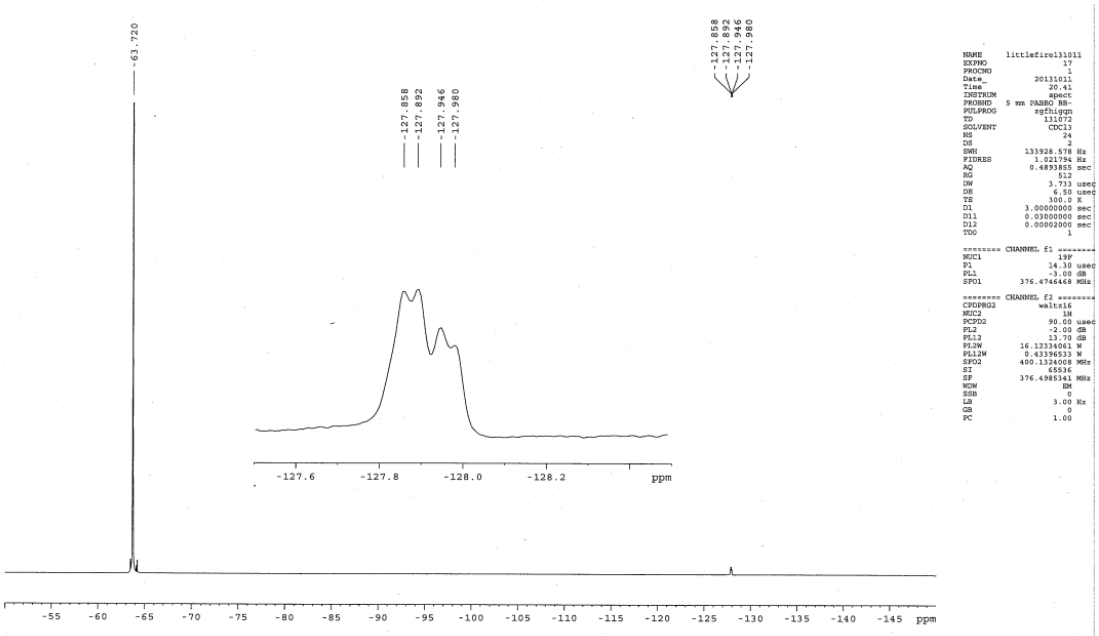

Fig. S37 ^{19}F NMR spectrum of **3** in $CDCl_3$

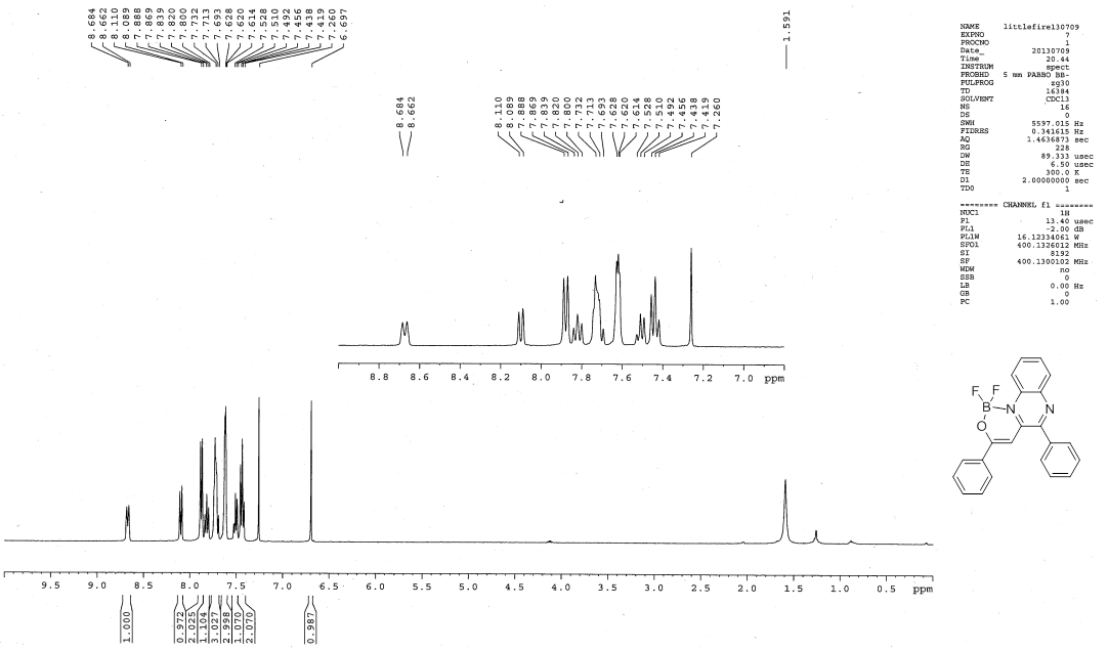

Fig. S38 ^{1}H NMR spectrum of **4** in $CDCl_3$

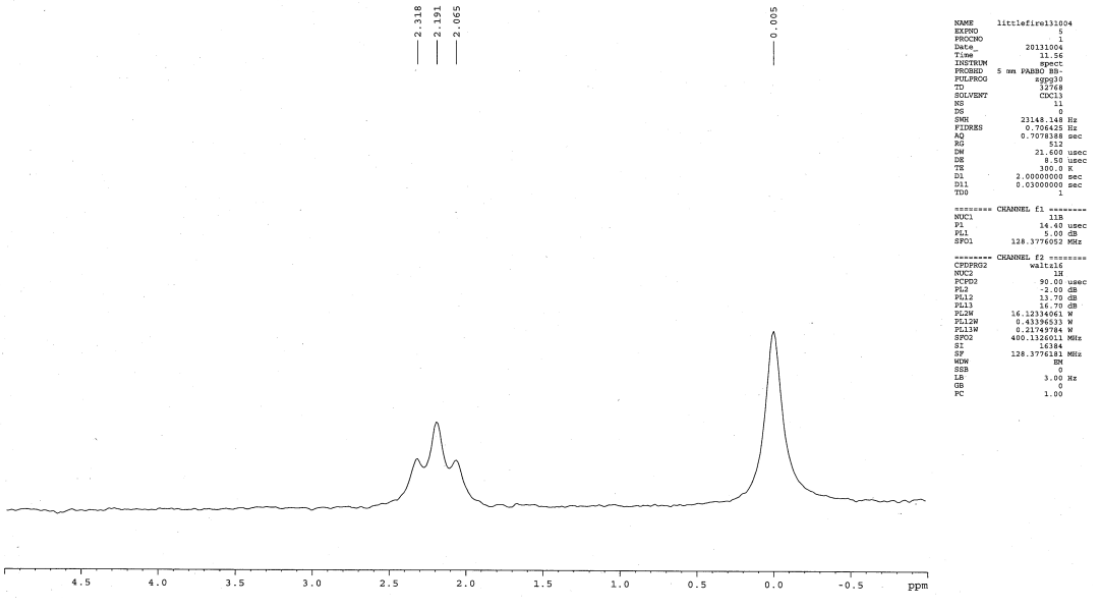

Fig. S39 ^{11}B NMR spectrum of **4** in $CDCl_3$

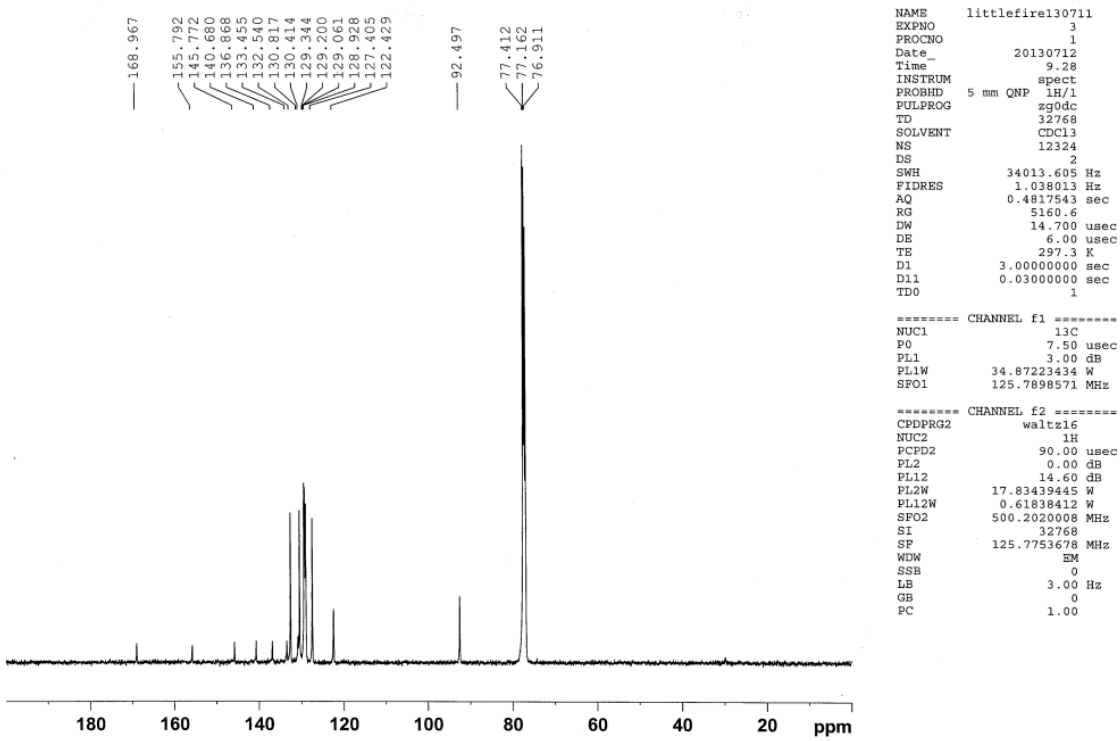

Fig. S40 ^{13}C NMR spectrum of **4** in $CDCl_3$

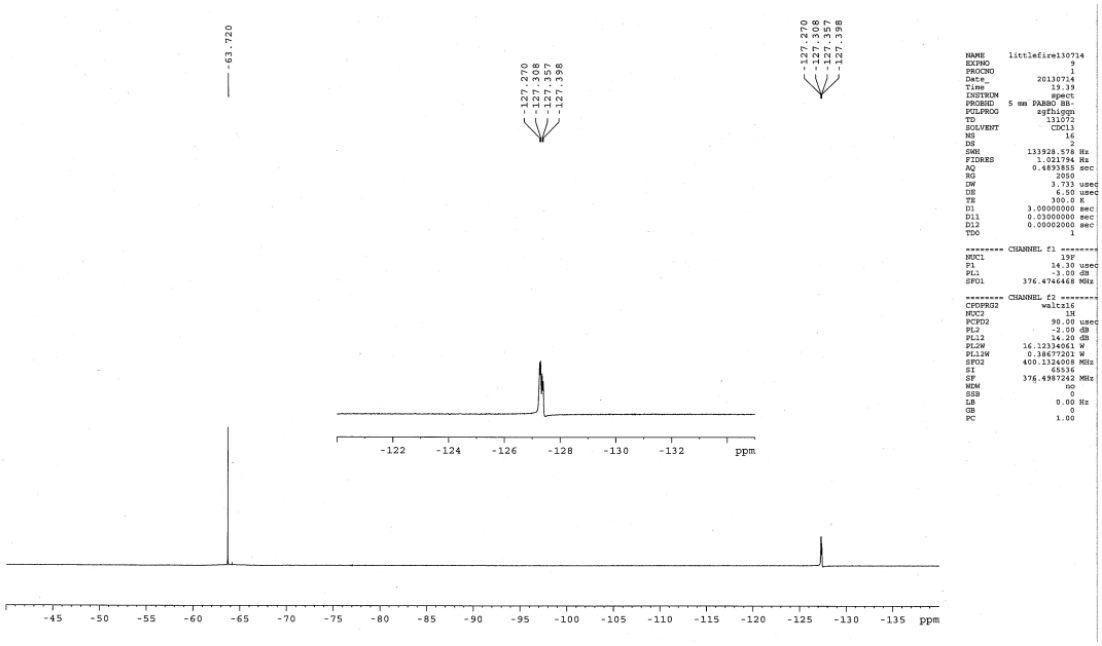

Fig. S41 ^{19}F NMR spectrum of **4** in $CDCl_3$

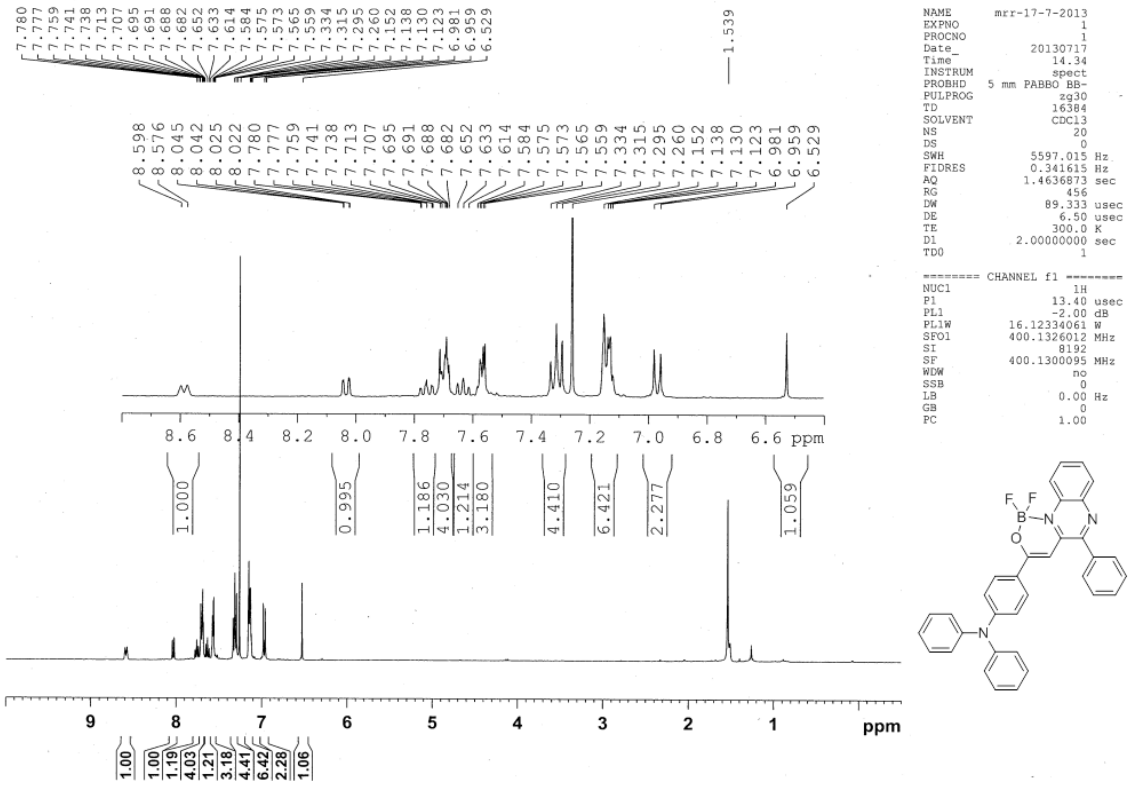

Fig. S42 ^{1}H NMR spectrum of **5** in $CDCl_3$

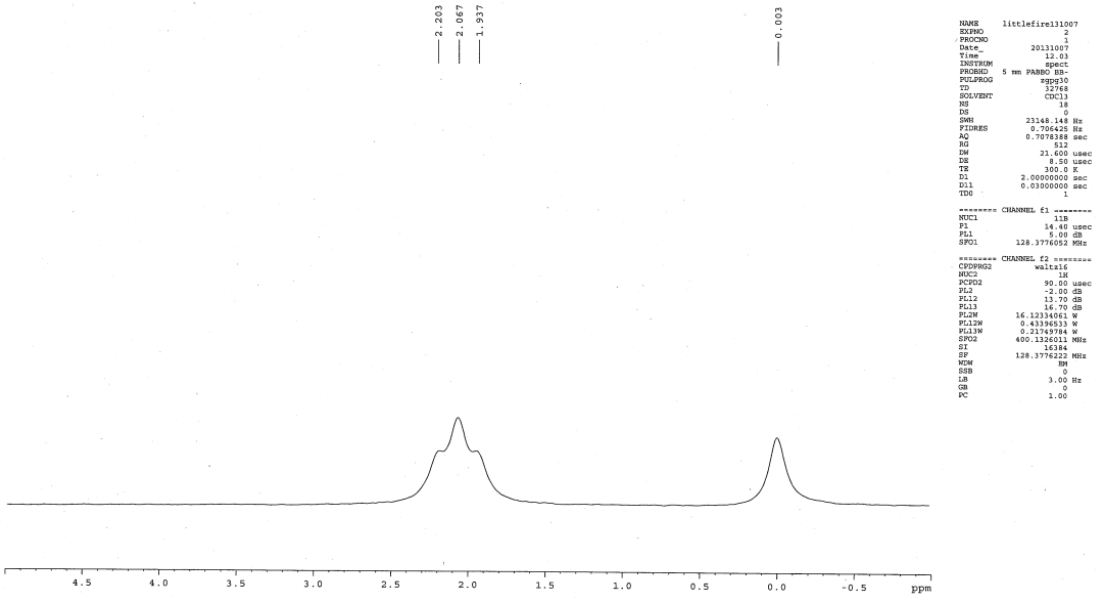

Fig. S43 ^{11}B NMR spectrum of **5** in $CDCl_3$

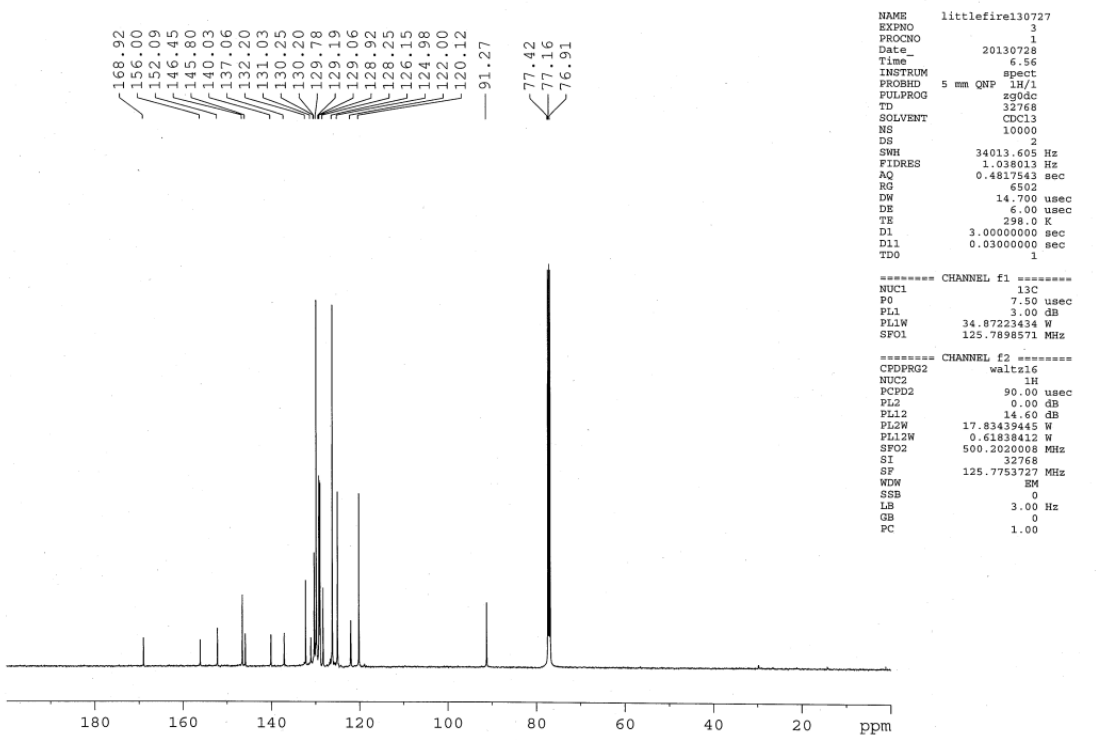

Fig. S44 ^{13}C NMR spectrum of **5** in $CDCl_3$

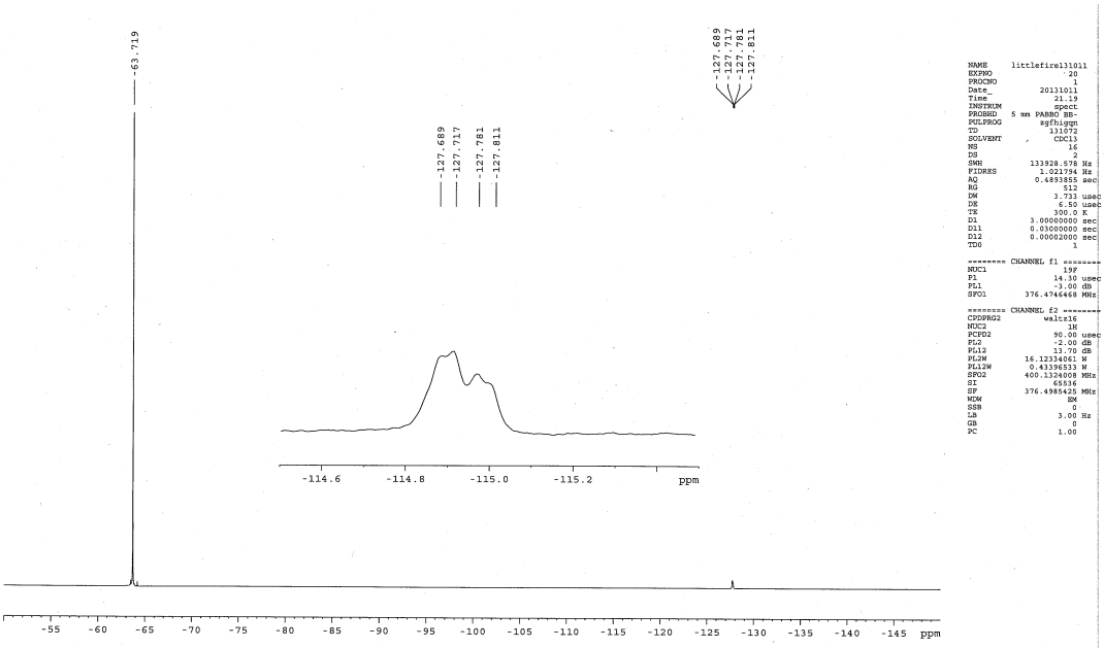

Fig. S45 ^{19}F NMR spectrum of **5** in $CDCl_3$